2018

Cytochrome c is an oxidative stress–activated plasmalogenase that cleaves plasmenylcholine and plasmenylethanolamine at the sn-1 vinyl ether linkage

Christopher M. Jenkins

Kui Yang

Gaoyuan Liu

Sung Ho Moon

Beverly G. Dilthey

See next page for additional authors

Authors
Christopher M. Jenkins, Kui Yang, Gaoyuan Liu, Sung Ho Moon, Beverly G. Dilthey, and Richard W. Gross

JBC EDITORS' PICK

Cytochrome *c* is an oxidative stress–activated plasmalogenase that cleaves plasmenylcholine and plasmenylethanolamine at the *sn*-1 vinyl ether linkage

Received for publication, December 21, 2017, and in revised form, February 22, 2018 Published, Papers in Press, March 12, 2018, DOI 10.1074/jbc.RA117.001629

Christopher M. Jenkins[‡§], **Kui Yang**[‡1], **Gaoyuan Liu**[‡§¶], **Sung Ho Moon**[‡§], **Beverly G. Dilthey**[‡§], **and Richard W. Gross**[‡§¶‖2]

From the [‡]*Division of Bioorganic Chemistry and Molecular Pharmacology and Departments of* [§]*Medicine and* [‖]*Developmental Biology, Washington University School of Medicine, St. Louis, Missouri 63110 and the* [¶]*Department of Chemistry, Washington University, St. Louis, Missouri 63130*

Edited by George M. Carman

Plasmalogens are phospholipids critical for cell function and signaling that contain a vinyl ether linkage at the *sn*-1 position and are highly enriched in arachidonic acid (AA) at the *sn*-2 position. However, the enzyme(s) responsible for the cleavage of the vinyl ether linkage in plasmalogens has remained elusive. Herein, we report that cytochrome *c*, in the presence of either cardiolipin (CL), O_2 and H_2O_2, or oxidized CL and O_2, catalyzes the oxidation of the plasmalogen vinyl ether linkage, promoting its hydrolytic cleavage and resultant production of 2-AA-lysolipids and highly reactive α-hydroxy fatty aldehydes. Using stable isotope labeling in synergy with strategic chemical derivatizations and high-mass-accuracy MS, we deduced the chemical mechanism underlying this long sought-after reaction. Specifically, labeling with either $^{18}O_2$ or $H_2{}^{18}O$, but not with $H_2{}^{18}O_2$, resulted in M + 2 isotopologues of the α-hydroxyaldehyde, whereas reactions with both $^{18}O_2$ and $H_2{}^{18}O$ identified the M + 4 isotopologue. Furthermore, incorporation of ^{18}O from $^{18}O_2$ was predominantly located at the α-carbon. In contrast, reactions with $H_2{}^{18}O$ yielded ^{18}O linked to the aldehyde carbon. Importantly, no significant labeling of 2-AA-lysolipids with $^{18}O_2$, $H_2{}^{18}O$, or $H_2{}^{18}O_2$ was present. Intriguingly, phosphatidylinositol phosphates (PIP_2 and PIP_3) effectively substituted for cardiolipin. Moreover, cytochrome *c* released from myocardial mitochondria subjected to oxidative stress cleaved plasmenylcholine in membrane bilayers, and this was blocked with a specific mAb against cytochrome *c*. Collectively, these results identify the first plasmalogenase in biology, reveal the production of previously unanticipated signaling lipids by cytochrome *c*, and present new perspectives on cellular signaling during oxidative stress.

Plasmalogens are phospholipids that contain a *cis*-vinyl ether linkage at the *sn*-1 position of the glycerol backbone and are essential for physiologic cellular function (1, 2). Typically, plasmalogens are highly enriched in polyunsaturated fatty acids, especially arachidonic acid, at the *sn*-2 position (3, 4). The unique properties of plasmalogens influence membrane structure and molecular dynamics, modulate the function of integral membrane proteins, and contribute to the phospholipase-mediated release of signaling fatty acids during cellular stimulation (5–9). Deficiencies in plasmalogen content have identified important roles for these specialized phospholipids in modulating signal transduction (10), cell proliferation (11), cholesterol trafficking (12), and sensitivity to oxidative stress (13, 14). Moreover, human genetic mutations leading to deficiencies in plasmalogen biosynthesis (*e.g.* PEX7 and alkylglycerone phosphate synthase (AGAPS)) unambiguously demonstrate that the absence of plasmalogens results in severe human disease (15–17). However, the cellular mechanisms mediating these phenomena, the enzymes that catalyze the cleavage of the *sn*-1 vinyl ether in plasmalogens (plasmalogenases), and mechanistic identification of the biologic functions of plasmalogens have remained largely enigmatic.

Mammalian myocardium contains substantial amounts of plasmalogens (>25% of total myocardial phospholipids and >60% of sarcolemmal phospholipids) that are highly enriched in arachidonic acid (AA)[3] at the *sn*-2 position. Furthermore, plasmalogen molecular species contain the majority of AA in many human cell types. Accordingly, delineation of the molec-

This work was supported by National Institutes of Health Grants RO1HL118639 and RO1HL133178. R. W. G. has financial relationships with LipoSpectrum and Platomics. The content is solely the responsibility of the authors and does not necessarily represent the official views of the National Institutes of Health.
This article was selected as one of our Editors' Picks.
This article contains Figs. S1–S4.

[1] Present address: Division of Pharmaceutical Analysis, U. S. Food and Drug Administration, St. Louis, MO 63110.
[2] To whom correspondence should be addressed: Washington University School of Medicine, Division of Bioorganic Chemistry and Molecular Pharmacology, 660 S. Euclid Ave., Campus Box 8020, St. Louis, MO 63110. Tel.: 314-362-2690; Fax: 314-362-1402; E-mail: rgross@wustl.edu.

[3] The abbreviations used are: AA, arachidonic acid; BOA, *O*-benzylhydroxylamine; CL, cardiolipin; cyt *c*, cytochrome *c*; 2-AA-LPC, 2-arachidonoyl-lysophosphatidylcholine; 2-AA-LPE, 2-arachidonoyl-lysophosphatidylethnaolamine; DMG, dimethylglycine; DTPA, diethylene triamine pentaacetic acid; ESI, electrospray ionization; HRAM, high-resolution accurate-mass; LUV, large unilamellar vesicle; plasmenyl-SAPC, 1-*O*-1′-(*Z*)-octadecenyl-2-arachidonoyl-*sn*-glycero-3-phosphocholine; plasmenyl-SAPE, 1-*O*-1′-(*Z*)-octadecenyl-2-arachidonoyl-*sn*-glycero-3-phosphoethanolamine; SUV, small unilamellar vesicle; PI(4,5)P_2, phosphatidylinositol 4,5-bisphosphate; PI(3,4,5)P_3, phosphatidylinositol 3,4,5-trisphosphate; POPC, 1-palmitoyl-2-oleoyl-*sn*-glycero-3-phosphocholine; PC, phosphatidylcholine; PE, phosphatidylethanolamine; SR, sarcoplasmic reticulum; AD, Alzheimer's disease; MIB, mitochondrial isolation buffer; 14:1 PC, 1,2-dimyristoleoyl-*sn*-glycero-3-phosphocholine; 16:1 PE, 1,2-dipalmitoleoyl-*sn*-glycero-3-phosphoethanolamine; Fmoc, fluorenylmethoxycarbonyl; COX, cyclooxygenase.

ular pathways mediating the cellular metabolism of plasmalogens is of paramount importance to understand their roles in cellular functions. However, despite intense efforts, an enzyme catalyzing the cleavage of the vinyl ether linkage in plasmenylcholine or plasmenylethanolamine, plasmalogenase, has eluded identification for nearly a century.

Oxidative stress is a major participant in mediating many of the pathologic processes present in diabetic cardiomyopathy, myocardial infarction/reperfusion, and the progression of heart failure (18–20). Mitochondria occupy over 30% of cardiac volume (21) and are the primary source of reactive oxygen species generated during myocardial ischemia/reperfusion injury (22–25). Furthermore, during ischemia/reperfusion, rapid changes in mitochondrial membrane potential and permeabilization (or rupture) of the outer membrane occur, leading to the release of cytochrome *c* (cyt *c*) (26–28). The release of cyt *c* from the intermembrane space allows its access to multiple signaling proteins, scaffolding complexes, and distal intracellular membrane compartments (29–31).

Under physiologic conditions, cyt *c* is bound to the inner mitochondrial membrane where it transfers electrons from complex III to complex IV. As an electron transfer protein, cyt *c* possesses a high redox potential (+260 mV) and a compact tertiary structure containing a covalently bound heme iron. Upon interaction with negatively charged phospholipids (32), especially cardiolipin (33), cyt *c* undergoes a conformational alteration with subsequent displacement of the axial Met-80 that is accompanied by a dramatic decrease in its redox potential to −400 mV. This prevents cyt *c* from serving as an electron transporter and allows access of hydrogen peroxide (produced by mitochondrial superoxide dismutase) to the heme moiety, conferring peroxidase activity to the conformationally altered cyt *c*. Previous work has shown that cardiolipin (CL)-bound cytochrome *c* can oxidize the polyunsaturated linoleoyl acyl chains in cardiolipin (34, 35), which can subsequently be released by calcium-independent phospholipase $A_2\gamma$ (36).

Based upon the known chemical sensitivity of the plasmalogen vinyl ether linkage to oxidation (37), we hypothesized that the peroxidase activity of cardiolipin-activated cytochrome *c* could oxidatively metabolize the vinyl ether bond in plasmalogens, leading to an intermediate that was susceptible to hydrolytic cleavage. Herein, we report that CL-activated cyt *c* catalyzes the oxidatively enabled hydrolytic cleavage of the vinyl ether linkage of plasmenylcholine and plasmenylethanolamine in the presence of H_2O_2 or alternatively by oxidized CL. The products of the reaction, 2-acyl-lysophospholipids and α-hydroxy fatty aldehydes, were identified either directly by high-resolution accurate-mass (HRAM) MS and fragmentation analyses or through synergistic chemical derivatization strategies and HRAM MS of derivatized precursor ions and their fragmentation-induced product ions. Importantly, we demonstrate that oxidized CL can activate the plasmalogenase activity of cyt *c* even in the absence of H_2O_2. To the best of our knowledge, this is the first identification of a protein that can catalyze the cleavage of the vinyl ether linkage of plasmalogens, thereby identifying multiple previously unknown cellular lipid metabolic pathways that participate in cellular metabolism, signaling, and cell fate decisions.

Results

Conformationally altered cytochrome c is a potent plasmalogenase

Because CL-activated cytochrome *c* is a potent lipid peroxidase in the presence of H_2O_2 (38), based upon energetic and molecular orbital considerations, we hypothesized that cyt *c* could catalyze the cleavage of the vinyl ether linkage present in plasmalogens. To test this hypothesis, we purified equine heart cytochrome *c* from Sigma by Mono S FPLC using an NaCl gradient. The purified cyt *c* migrated as a single band by SDS-PAGE and was >99% pure by silver staining (Fig. S1). The purified cyt *c* was incubated with small unilamellar vesicles (SUVs) comprising 1-*O*-1′-(*Z*)-octadecenyl-2-arachidonoyl-*sn*-glycero-3-phosphocholine (plasmenyl-SAPC) as host containing 10 mol % bovine heart CL (predominantly tetra-18:2 CL) as guest in the absence or presence of H_2O_2 for 10 min at 37 °C. We focused on CL because it is markedly enriched in mitochondria and has been previously demonstrated to bind to cyt *c* inducing a conformational change that activates its cryptic peroxidase activity (34, 39–42). In initial experiments, reactions were monitored for the production of LPC by shotgun lipidomics. Minimal plasmalogenase activity was observed in the absence or presence of H_2O_2 alone (Fig. 1*A*). Similarly, incubations with cyt *c* alone also resulted in barely detectable cleavage of the plasmenylcholine vinyl ether linkage (minor peak at *m/z* 566.4 by ESI-MS/MS) (Fig. 1*A*). Addition of H_2O_2 dramatically activated cyt *c* plasmalogenase activity, resulting in the robust generation of 2-AA-LPC (Fig. 1*A*). In contrast, similar experiments with diacyl SAPC-CL SUVs did not result in appreciable production of either 1-stearoyl-LPC or 2-AA-LPC in the presence of cyt *c* and H_2O_2 (data not shown). Incubation of SUVs comprising 1-*O*-1′-(*Z*)-octadecenyl-2-arachidonoyl-*sn*-glycero-3-phosphoethanolamine (plasmenyl-SAPE) (45 mol %) containing 1-palmitoyl-2-oleoyl-*sn*-glycero-3-phosphocholine (POPC) (45 mol %) and 10 mol % bovine heart CL in the presence of cyt *c* resulted in the production of 2-AA-LPE, which was markedly increased in the presence of H_2O_2 (Fig. 1*B*).

Substantiation of cytochrome c as a plasmalogenase

Further characterization of the plasmalogenase activity of cytochrome *c* revealed that production of 2-AA-LPC from plasmenyl-SAPC depended upon the amount of purified cytochrome *c* (Fig. 2*A*) with a maximum apparent turnover number of ≈6 at low concentrations of cyt *c* (1 μM). The reaction was also dependent on the concentration of H_2O_2 (Fig. S2A) as well as on the mol % cardiolipin present in the host plasmenyl-SAPC vesicles (Fig. S2B). Kinetic analysis of reaction products at a fixed concentration of cytochrome *c* (5 μM) in the presence of H_2O_2 (200 μM) demonstrated a linear increase in 2-AA-LPC and 2-AA-LPE production utilizing plasmenyl-SAPC/1-palmitoyl-2-oleoyl-*sn*-glycero-3-phosphoethanolamine or plasmenyl-SAPE/POPC SUVs, respectively, each containing 10 mol % CL as guest to mimic physiologic conditions (Fig. S2C). The initial catalytic rates of vinyl ether cleavage were ~50 nmol of 2-AA-LPC/min·mg of cyt *c* and ~60 nmol of 2-AA-LPE/min·mg of cyt *c*.

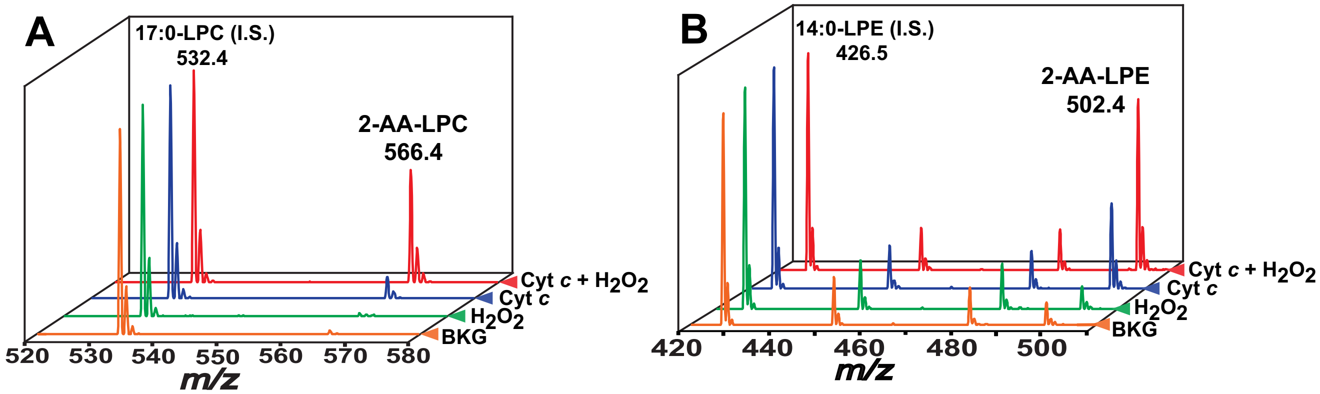

Figure 1. Mass spectrometric analyses of the plasmalogenase reaction products. *A*, plasmenyl-SAPC/CL (50 nmol/5 nmol) SUVs in 200 μl were incubated in the presence of cytochrome *c* (10 μM) and/or H_2O_2 (250 μM) or in the absence of both (*BKG*) for 10 min at 37 °C. Following addition of 17:0 LPC (*m/z* 532.4) as internal standard (*I.S.*), resultant lipids were extracted into chloroform (Bligh-Dyer extraction) and directly analyzed by ESI-MS/MS in the positive-ion mode through tandem mass spectrometric analysis through neutral loss scanning at *m/z* 59 for sodiated LPC species as described previously (71). *B*, plasmenyl-SAPE (45 mol %) in POPC (45 mol %) SUVs containing 10 mol % CL were incubated in the presence of cyt *c* and/or H_2O_2 or in the absence of H_2O_2 and cyt *c* (*BKG*) at 37 °C for 10 min. Following addition of internal standard (14:0 LPE; *m/z* 426.5), reaction products were extracted and directly analyzed by ESI-MS in the positive-ion mode through mass spectrometric analysis of protonated LPE species as described previously (86).

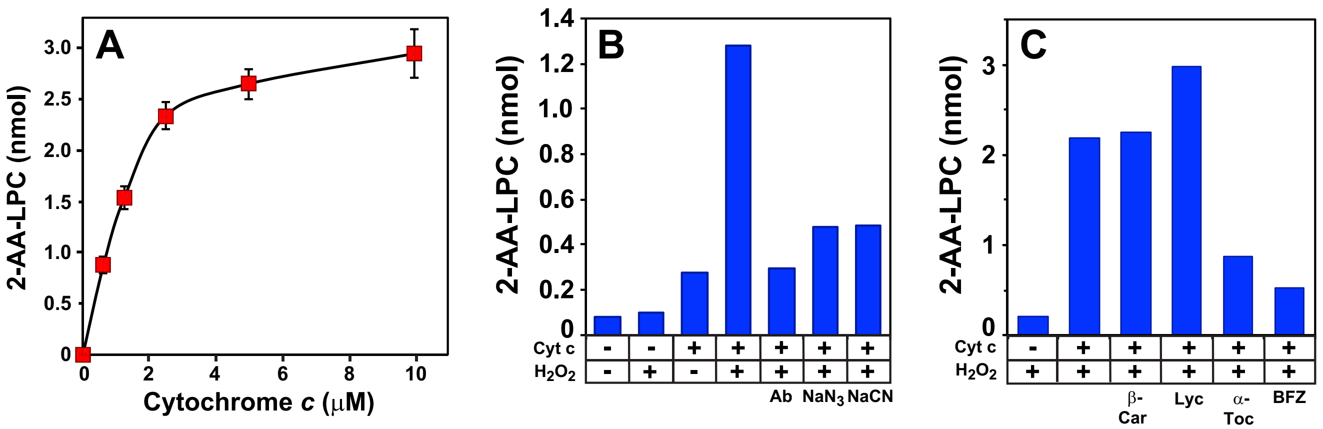

Figure 2. Dependence of plasmalogenase activity on cytochrome *c* and susceptibility of the cyt *c* plasmalogenase reaction to various inhibitors. *A*, cytochrome *c* at the indicated concentrations was incubated with plasmenyl-SAPC (250 μM)/CL (25 μM) SUVs in the presence of H_2O_2 (250 μM) in 10 mM potassium phosphate, pH 7.0, containing 0.25 mM DTPA (200-μl reaction volume) for 10 min at 37 °C. *Error bars* represent S.E. of at least three separate experiments. *B*, inhibition of cytochrome *c* plasmalogenase activity with either an anti-cytochrome *c* mAb (*Ab*), NaN_3 (2 mM), or NaCN (2 mM). The mAb directed against cyt *c* was preincubated with cyt *c* prior to the assay for plasmalogenase activity. *C*, effect of singlet oxygen scavengers β-carotene (β-*Car*) and lycopene (*Lyc*), the lipid peroxyl radical scavenger α-tocopherol (α-*Toc*), or the cytochrome P450 inhibitor bifonazole (*BFZ*) on the plasmalogenase activity of cytochrome *c*. Following addition of internal standards (17:0 LPC and 14:1 PC), reaction products were extracted and analyzed as described under "Experimental procedures."

We next examined the susceptibility of the plasmalogenase reaction to various inhibitors. Importantly, a cyt *c*–specific mAb resulted in the nearly complete inhibition of H_2O_2-dependent cyt *c* plasmalogenase activity (Fig. 2*B*). Moreover, cyanide and azide inhibited the plasmalogenase activity as has been shown for inhibition of the peroxidase activity of cyt *c* (43, 44) (Fig. 2*B*). Although the singlet oxygen scavengers lycopene and β-carotene did not appreciably affect cyt *c*–mediated plasmalogenase activity, the lipid hydroperoxyl scavenger α-tocopherol markedly inhibited the measured plasmalogenase activity (Fig. 2*C*). Interestingly, bifonazole, a cytochrome P450 inhibitor that inhibits the peroxidase activity of cyt *c* (45), potently inhibited cyt *c*–mediated plasmalogenase activity (Fig. 2*C*). To rule out the possible contribution of free heme or free iron to the observed plasmalogenase activity, hemin or ferric chloride was substituted for cyt *c* in the presence of hydrogen peroxide. Incubations with these reagents did not result in appreciable plasmalogenase activity (Fig. S3A). Additional experiments with catalase and nitric-oxide synthase revealed that these heme proteins exhibited <10% and no plasmalogenase activity compared with cyt *c*, respectively (Fig. S3B), suggesting that cytochrome *c* is relatively specific for cleavage of the plasmalogen vinyl ether linkage. We specifically point out that these results do not preclude the possibility that other heme proteins may also be capable of cleaving the plasmalogen vinyl ether bond. Collectively, these results firmly identify cytochrome *c* as an enzymic mediator of the cleavage of the plasmalogen vinyl ether linkage.

Identification of the regiospecificity of the lysolipid reaction products from plasmenylcholine and plasmenylethanolamine

To establish the regiospecificity of the arachidonoyl moiety in the lysolipids produced by cyt *c*–catalyzed plasmalogenase activity, full-mass MS^2 analyses of the lysolipid products and authentic synthetic 2-AA-LPC and 2-AA-LPE standards were compared. Excellent matches of the full-mass MS^2 spectra

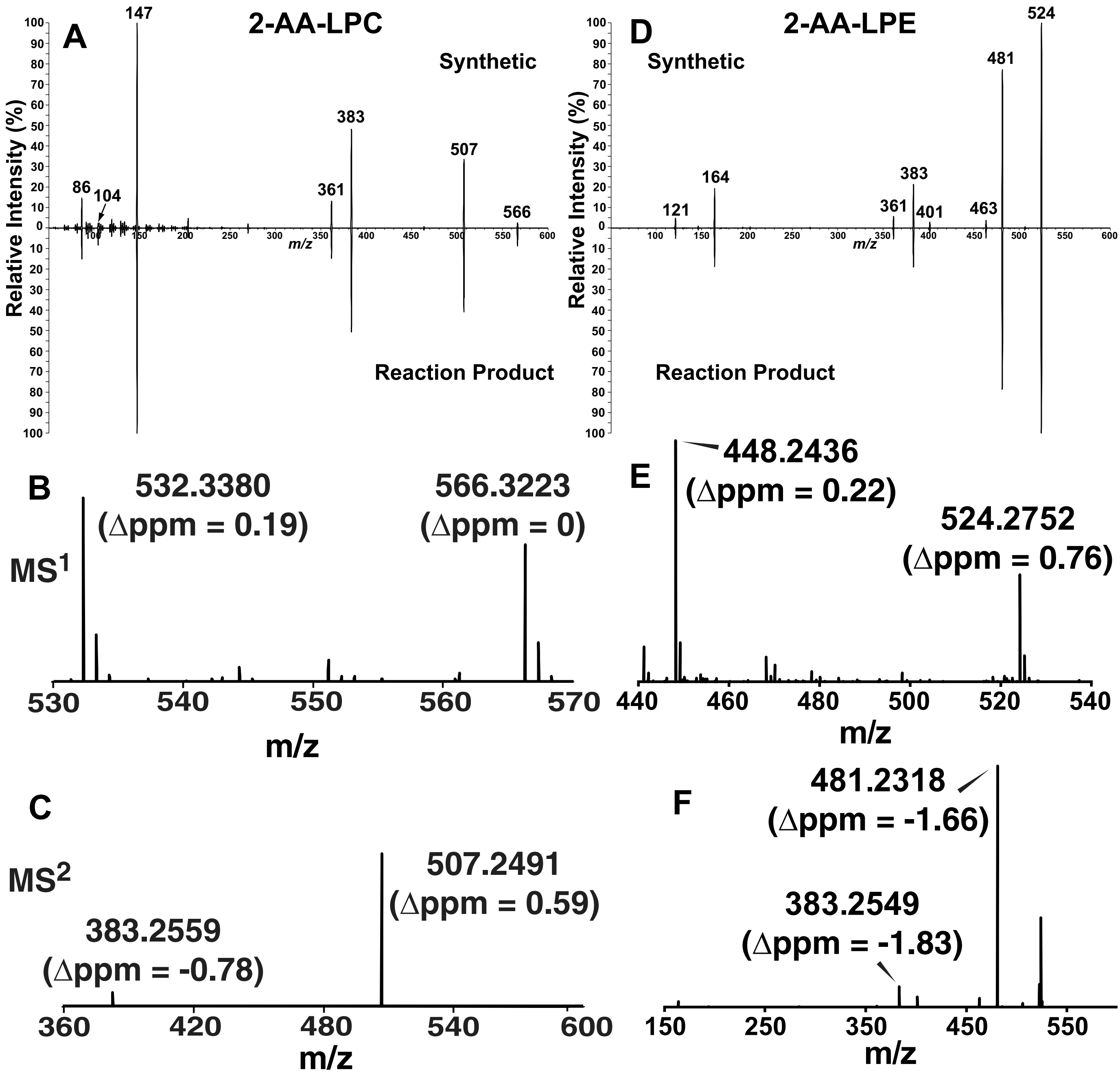

Figure 3. Mass spectrometric structural confirmation of 2-AA-LPC and 2-AA-LPE generated from plasmenyl-SAPC and plasmenyl-SAPE by the plasmalogenase activity of cytochrome *c* in the presence of H_2O_2. *A*, full-mass MS^2 analysis of both plasmalogenase assay product and synthetic 2-AA-LPC at *m/z* 566.2 was performed on a triple-quadrupole mass spectrometer. An excellent match of the two MS^2 spectra are displayed as a mirror plot, including the presence of high-abundance product ion at *m/z* 147.1 (*i.e.* sodiated ethylene phosphate), which indicates the regiospecific acylation at the *sn*-2 position of LPC species (71). *B* and *C*, HRAM MS^1 and MS^2 mass spectrometric analysis of the assay product at *m/z* 566.3223 from *A* was also performed on an LTQ-Orbitrap mass spectrometer. The measured *m/z* values of the product ions (at *m/z* 507.2491 and 383.2559) resulting from loss of trimethylamine and phosphocholine, respectively, confirm the identity of the phosphocholine headgroup in LPC with each within ±2 ppm of theoretical values. In *panel B*, the peak corresponding to *m/z* 532.3380 is the 17:0 LPC internal standard. *D*, MS^2 analysis of both the plasmalogenase assay product and synthetic 2-AA-LPE at *m/z* 524 (sodium adduct) was performed on a triple-quadrupole mass spectrometer. The MS^2 spectra demonstrate the presence of diagnostic fragment ions (prominent *m/z* 164 (sodiated phosphoethanolamine) and *m/z* 383 (sodiated arachidonoyl glycerol) peaks) indicative of 2-AA-LPE (46). *E* and *F*, HRAM MS^1 and MS^2 mass spectrometric analysis of the assay product at *m/z* 524.2752 from *D* was also performed on an LTQ-Orbitrap mass spectrometer showing fragment ions corresponding to the accurate mass ±2 ppm of the aforementioned product ions. In *panel E*, the peak corresponding to *m/z* 448.2436 is the 14:0 LPE internal standard.

(shown as mirror plots) were obtained between the lysolipid reaction products and corresponding authentic 2-AA-LPC and 2-AA-LPE standards (Fig. 3, *A* and *D*). For 2-AA-LPC, the presence of a high abundance product ion at *m/z* 147.1 (*i.e.* sodiated ethylene phosphane) demonstrated the regiospecificity of the arachidonate group at the *sn*-2 position as described previously (46). We also performed high-mass-accuracy MS^1 and MS^2 analyses of the 2-AA-LPC and 2-AA-LPE assay products by HRAM MS. Each of the measured masses of the molecular ion and product ions for 2-AA-LPC and 2-AA-LPE were within ±2

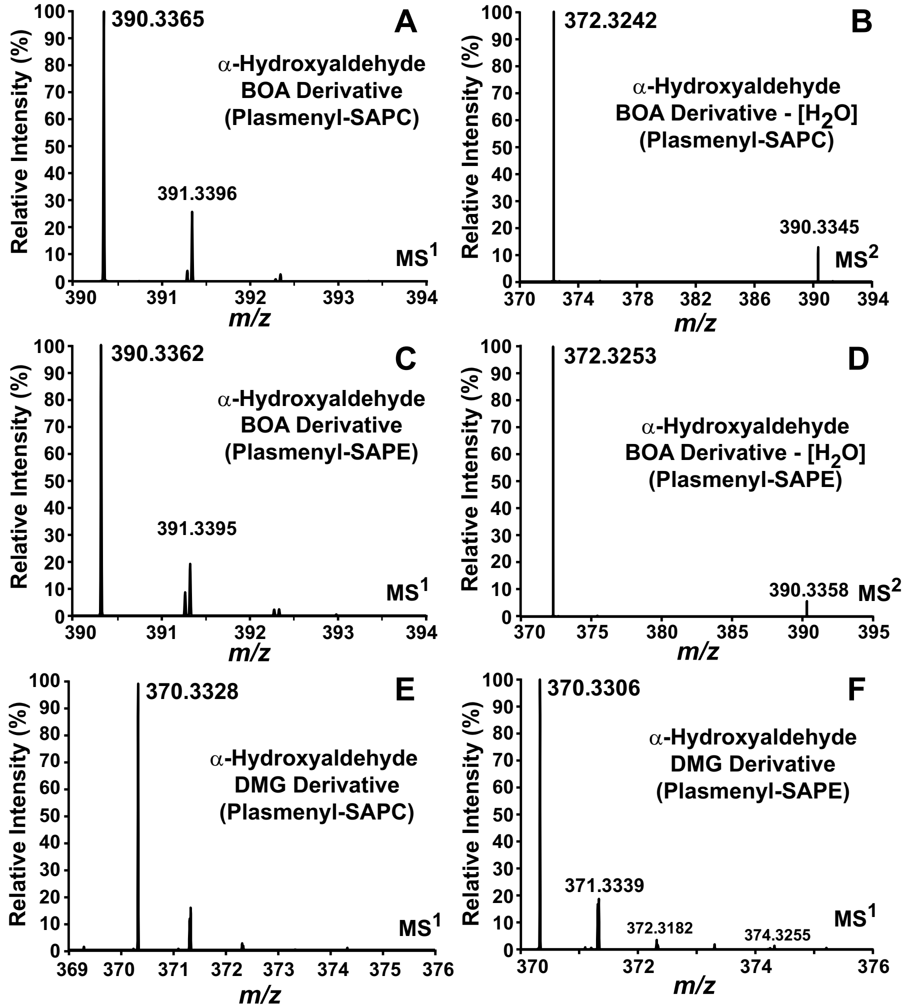

Figure 4. Mass spectrometric identification of α-hydroxyaldehyde products in cytochrome *c*–catalyzed plasmalogenase reactions. Plasmenyl-SAPC/POPC (*A*, *B*, and *E*) or plasmenyl-SAPE/POPC (*C*, *D*, and *F*) vesicles containing 10 mol % bovine heart CL (predominantly tetra-18:2 CL) were incubated at 37 °C for 30 min in the presence of cyt *c* (20 μM) and H_2O_2 (200 μM). Aliphatic α-hydroxyaldehydes were extracted into cyclohexane/diethyl ether (4:1) and derivatized with either BOA or DMG. Derivatives were analyzed by HRAM MS. MS^2 product ion scans of the C18:0 α-hydroxyaldehyde derivatized with BOA (*m/z* 390.336) in *B* and *D* show a product ion peak at *m/z* 372.325 upon neutral loss of H_2O.

ppm of their calculated theoretical masses (Fig. 3, *B, C, E,* and *F*).

Identification of the oxidized sn-1 chain aliphatic constituents

To determine the reaction products resulting from oxidative cleavage of the vinyl ether bond, we utilized synergistic derivatization strategies to avoid the rapid postsource decay of the anticipated aldehyde reaction products. After incubation of cyt *c* with plasmenyl-SAPC/CL (90:10) SUVs in the presence of H_2O_2, the resultant aldehydes were derivatized with *O*-benzylhydroxylamine (BOA). High-mass-accuracy MS spectra of aldehyde BOA derivatives demonstrated an intense molecular ion at *m/z* 390.3365 (Fig. 4*A*), indicative of the anticipated product of the C18:0 α-hydroxyaldehyde BOA adduct. Fragmentation of the molecular ion at *m/z* 390.3365 resulted in the appearance of a predominant peak at 372.3242 resulting from loss of H_2O (Fig. 4*B*). Similar BOA derivative ions were obtained when plasmenyl-SAPE/POPC/CL vesicles were used as substrate (Fig. 4, *C* and *D*). To further confirm the presence of the hydroxyl group in the resultant aldehyde product, dimethylglycine (DMG) was used to derivatize the hydroxyl groups. An intense molecular ion at *m/z* 370.3328 corresponding to the mass of the C18:0 α-hydroxyaldehyde DMG derivative was routinely observed (Fig. 4*E*). Similar results were obtained when plasmenyl-SAPE was used as substrate (Fig. 4*F*). Collectively, these results demonstrate that cytochrome *c*–mediated oxidative cleavage of the vinyl ether bond of plasmalogens generates lysophospholipids and α-hydroxy fatty aldehydes as products.

Activation of cyt c–mediated plasmalogenase activity by oxidized CL alone or by phosphatidylinositol phosphates in the presence of H_2O_2

Because cardiolipin is likely oxidized by cyt *c* during the plasmalogenase reaction, we examined whether CL preoxidized with cyt *c* in the presence of H_2O_2 could activate the plasmalogenase activity of cyt *c* in the absence of exogenous H_2O_2 in the reaction mixture. First, cardiolipin was oxidized by cyt *c* in the presence of hydrogen peroxide (35). Second, oxidized CL molecular species were purified by HPLC and analyzed by

HRAM MS. Spectra revealed the presence of multiple oxidized molecular species with an approximate 1:1 mixture of hydroperoxides and hydroxides, similar to results described previously (35). Next, we incorporated the HPLC-purified cyt *c*–oxidized CL (10 mol %) as guests into plasmenyl-SAPC SUV hosts by sonication and then measured the plasmalogenase activity of cyt *c* using these SUVs as substrate containing oxidized CL in the absence of additional H_2O_2. Remarkably, inclusion of cyt *c*–oxidized CL fully reconstituted the plasmalogenase activity even in the absence of exogenous H_2O_2 (Fig. 5*A*, *upper panel*). Additionally, cyt *c*–catalyzed plasmalogenase activity could be further increased by the addition of H_2O_2 (Fig. 5*A*, *upper panel*). Previous reports have indicated that cytochrome *c* binds less tightly to oxidized CL compared with nonoxidized CL. We performed vesicle binding experiments with plasmenyl-SAPC large unilamellar vesicles (LUVs) containing either 1) no CL, 2) 10 mol % nonoxidized CL, or 3) 10 mol % oxidized CL. The results revealed that although cytochrome *c*

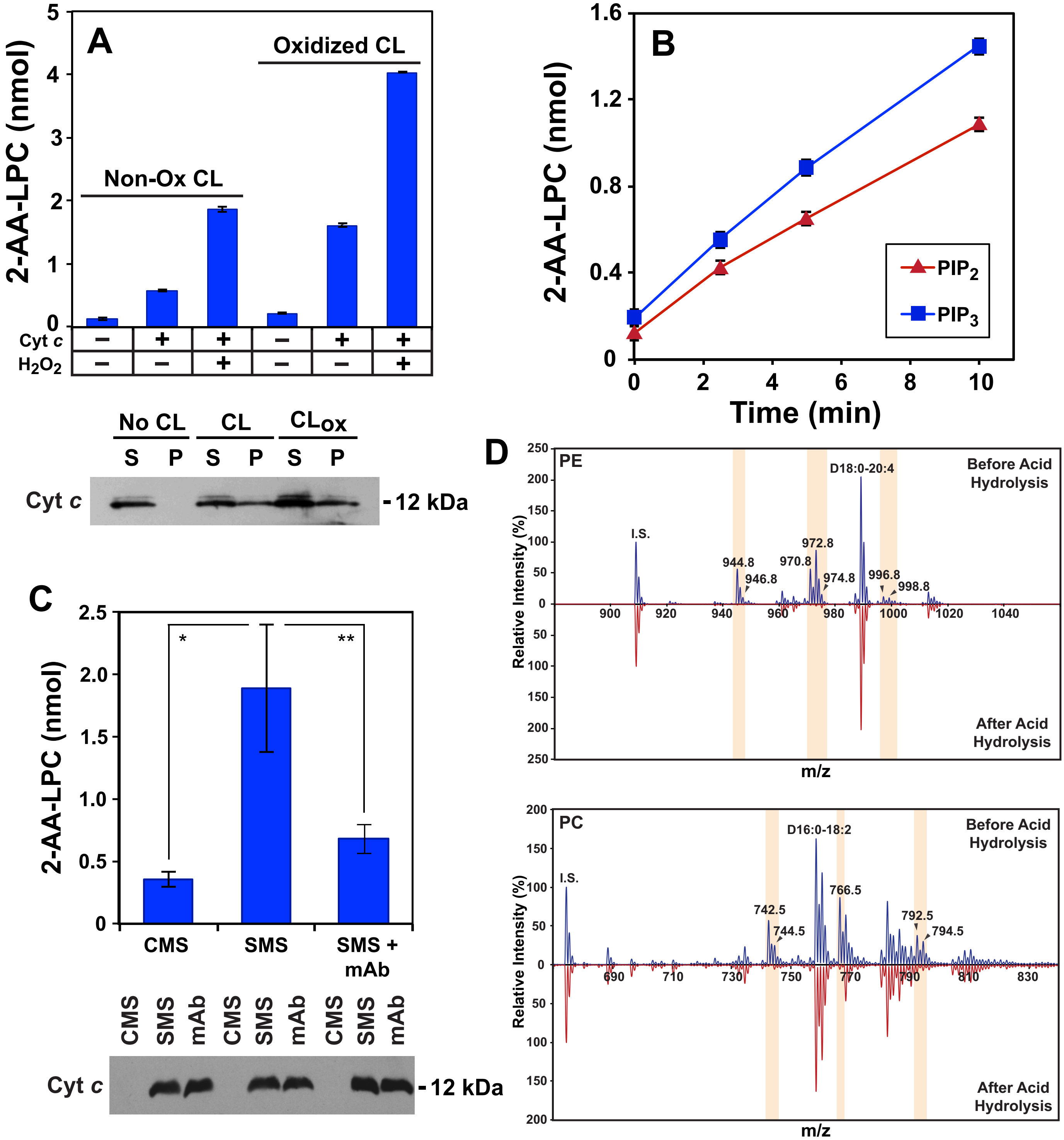

does not appreciably bind to vesicles in the absence of cardiolipin it readily binds to plasmenyl-SAPC LUVs containing either nonoxidized or oxidized CL (Fig. 5*A*, *lower panel*). These results are consistent with the CL-dependent activation of cyt *c* plasmalogenase activity (Fig. S2B).

Next, we hypothesized that other negatively charged phospholipids such as $PI(4,5)P_2$ and $PI(3,4,5)P_3$ (which are enriched in the plasma membrane) could also act to transform cyt *c* into a potent plasmalogenase after its release from the mitochondrial intermembrane space. Accordingly, we examined the ability of 5 mol % $PI(4,5)P_2$ or $PI(3,4,5)P_3$ as guests in host plasmenyl-SAPC SUVs in the presence of H_2O_2 to activate cyt *c* plasmalogenase activity. The results demonstrated robust activation of plasmalogenase activity with phosphatidylinositol phosphates similar to that observed with CL, suggesting that released cyt *c* activated by association with negatively charged lipids has multiple membrane targets after its release from the mitochondria (Fig. 5*B*).

Mitochondrial cytochrome c mediated plasmalogenase activity

Next, we examined whether cyt *c* released from rabbit heart mitochondria by outer membrane permeabilization could cleave the vinyl ether linkage of plasmenyl-SAPC in exogenous SUVs containing CL. Incubation of rabbit heart mitochondria in the presence of KCl and calcium phosphate resulted in swelling of the mitochondria and the robust release of cyt *c* as demonstrated by Western blot analysis of the mitochondrial supernatant with a specific anti-cyt *c* mAb (Fig. 5*C*). After removal of the mitochondria by centrifugation, the resultant supernatant was incubated with plasmenylcholine vesicles containing 10 mol % oxidized CL in the absence or presence of a specific mAb against cyt *c*. Similar to incubations with purified cyt *c*, addition of the anti-cyt *c* mAb to stressed rabbit heart mitochondrial supernatants resulted in marked inhibition of plasmalogenase activity, indicating that cyt *c* was responsible for the observed activity (Fig. 5*C*).

Human heart mitochondria contain abundant plasmalogen molecular species

Mammalian myocardium is known to be enriched in plasmalogen molecular species (7). Previously, subcellular fractionation and mass spectrometric analysis of phospholipids from canine myocardium revealed substantial enrichment of plasmalogens in sarcolemmal and sarcoplasmic reticular membranes (3, 4). To determine whether mitochondrial membranes contained plasmalogens representing a proximal target for cytochrome *c* plasmalogenase activity, we measured choline and ethanolamine plasmalogens in human heart mitochondria by shotgun lipidomics. The results demonstrated that human heart mitochondria contain an abundance of both ethanolamine and choline plasmalogens enriched in AA (Fig. 5*D*). These results strongly suggest that cytochrome *c* localized to human heart mitochondria generates plasmalogen-derived lipid second messengers during oxidative stress.

Metabolic labeling of cytochrome c plasmalogenase reaction products in the presence of $^{18}O_2$, $H_2{}^{18}O_2$, and/or $H_2{}^{18}O$

To gain insight into the chemical mechanisms through which cyt *c* catalyzes the cleavage of the vinyl ether linkage in the plasmalogenase reaction, we incubated cyt *c* with plasmenylcholine vesicles containing 10 mol % CL in the presence of either $^{18}O_2$, $H_2{}^{18}O$, $H_2{}^{18}O_2$, or $^{18}O_2$ and $H_2{}^{18}O$ together. The reaction products were derivatized with either BOA (for derivatization of aldehydes) (47) or DMG (for derivatization of hydroxyl groups). These reactions were each selected for the high ionization efficiency of their derivatives and their ability to substantiate the identities of the proposed reaction products (48). Control incubations of cyt *c* with 10 mol % oxidized CL/plasmenyl-SAPC vesicles in the presence of supplemental $^{16}O_2$ and $H_2{}^{16}O$ resulted in the appearance of a BOA adduct at m/z 390.3365 (Fig. 6*A*), which upon fragmentation yielded a diagnostic product ion at m/z 372.3242 consistent with loss of $H_2{}^{16}O$ (Fig. 7*A*). Substitution of $^{18}O_2$ for $^{16}O_2$ resulted in the formation of a BOA adduct containing one ^{18}O atom (m/z = 392.3387) (Fig. 6*B*), which upon fragmentation yielded a product ion at m/z 372.3241 (loss of $H_2{}^{18}O$ ($\Delta m/z = 20.0146$)) (Fig. 7*B*). Because derivatization of aldehydes with BOA results in loss of the aldehyde oxygen during formation of the oxime (47), one of the oxygen atoms in molecular oxygen must be incorporated into the aliphatic chain of the aldehyde product, likely as an α-hydroxyl group that readily loses water upon fragmentation. In contrast, reactions performed in $H_2{}^{18}O$ did not result in

Figure 5. Substitution of oxidized CL reconstitutes cytochrome *c*–mediated plasmalogenase activity in the absence of H_2O_2, binding of cyt *c* to plasmenyl-SAPC LUVs, kinetics of plasmalogenase activity in the presence of $PI(4,5)P_2$ or $PI(3,4,5)P_3$, hydrolysis of plasmenylcholine by cytochrome *c* released from rabbit heart mitochondria, and abundance of plasmalogens in human heart mitochondria. *A*, *upper panel*, plasmenyl-SAPC vesicles containing either 10 mol % bovine heart CL (predominantly tetra-18:2 CL) or bovine heart CL previously oxidized with cyt *c* and H_2O_2 (35) were incubated with cyt *c* (10 μM) in the presence or absence of H_2O_2 (200 μM) for 10 min at 37 °C. Reaction products extracted into chloroform (Bligh-Dyer) in the presence of 17:0 LPC internal standard were analyzed by tandem MS in the positive-ion mode. *Lower panel*, binding of cyt *c* to plasmenylcholine large unilamellar vesicles. Purified cyt *c* (2.5 μM final concentration) was mixed with plasmenyl-SAPC LUVs (0.8 μm) in the absence or presence of 10 mol % CL or 10 mol % oxidized CL (CL_{ox}) at 23 °C in 10 mM potassium phosphate, pH 7.0, containing 0.25 mM DTPA prior to ultracentrifugation (100,000 × *g* for 60 min) at 15 °C. Pellet (*P*) and supernatant (*S*) fractions were resolved by SDS-PAGE and visualized by ECL Western blot analysis as described under "Experimental procedures." *B*, plasmenyl-SAPC vesicles containing either 10 mol % $PI(4,5)P_2$ (*PIP_2*) or $PI(3,4,5)P_3$ (*PIP_3*) were incubated with cyt *c* (10 μM) in the presence of H_2O_2 (200 μM) for the indicated times. After addition of 17:0 LPC internal standard, resultant 2-AA-LPC was quantified by LC-MS. *Error bars* in *A* and *B* represent S.E. for at least three separate experiments. *C*, mitochondria were isolated from rabbit myocardium and incubated in sucrose-mannitol buffer in the absence (control) or presence of KCl and calcium phosphate to release cyt *c*. Following pelleting of swollen mitochondria by centrifugation, the resultant supernatants were incubated with plasmenyl-SAPC vesicles containing 10 mol % oxidized CL for 20 min at 37 °C under the indicated conditions. Following extraction into chloroform (Bligh-Dyer), 2-AA-LPC was quantified by tandem mass spectrometry using 17:0 LPC as an internal standard. Data presented are from two separate experiments performed in triplicate ($\bar{x}$ ± S.E., $n = 6$; *, $p < 0.02$; **, $p < 0.05$). The content of cyt *c* in the supernatant fractions was determined by ECL Western blot analysis. *CMS*, control mitochondrial supernatant; *SMS*, swollen mitochondrial supernatant; *mAb*, anti-cyt *c* mAb. *D*, PE (Fmoc-derivatized, *upper panel*) and PC (*lower panel*) plasmalogens present in human heart mitochondria. The presence of plasmenylcholine and plasmenylethanolamine molecular species (*beige shaded regions*) were confirmed by their sensitivity to acid hydrolysis. Major plasmenylethanolamine molecular species containing arachidonic acid are as follows (P represents plasmenyl): P16:0–20:4 PE (m/z 944.8), P18:1–20:4 PE (m/z 970.8), and P18:0–20:4 PE (m/z 972.8). Major plasmenylcholine molecular species containing arachidonic acid are as follows: P16:0–20:4 PC (m/z 766.5), P18:1–20:4 PC (m/z 792.5), and P18:0–20:4 PC (m/z 794.5). *I.S.*, internal standard.

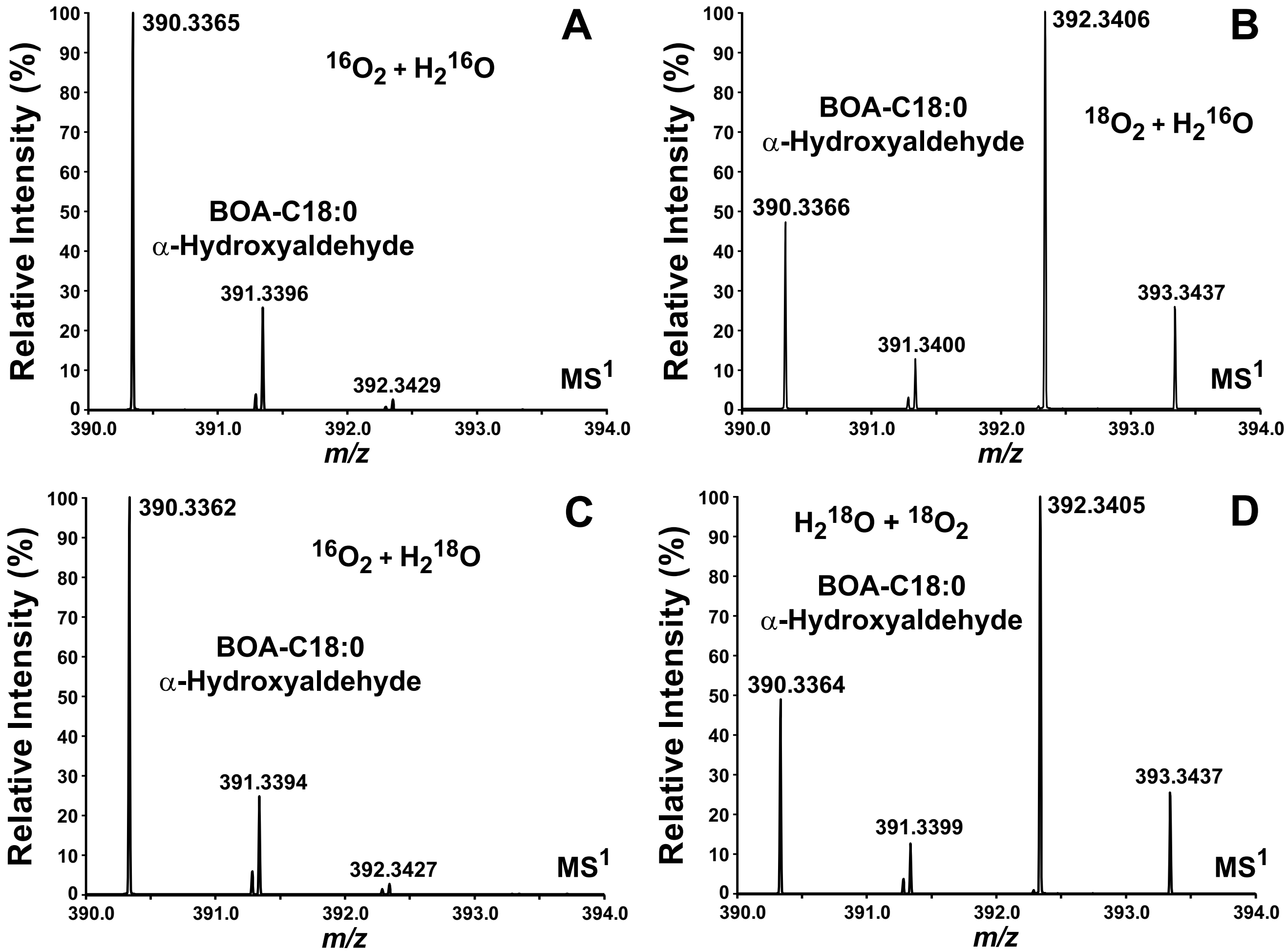

Figure 6. Incorporation of ^{18}O from $^{18}O_2$ into the BOA-derivatized α-hydroxyaldehyde product of the plasmalogenase reaction of cytochrome *c*. Plasmenyl-SAPC vesicles containing 10 mol % oxidized CL were incubated with cyt *c* in the presence of $^{16}O_2$ and $H_2{}^{16}O$ (*A*), $^{18}O_2$ and $H_2{}^{16}O$ (*B*), $^{16}O_2$ and $H_2{}^{18}O$ (*C*), or $^{18}O_2$ and $H_2{}^{18}O$ (*D*) for 30 min at 37 °C. Reaction products were extracted into cyclohexane/diethyl ether (4:1), derivatized with BOA, and analyzed by MS as described under "Experimental procedures." Peaks of BOA-derivatized α-hydroxyaldehydes labeled with ^{16}O or ^{18}O are shown at *m/z* 390.3365 or 392.3405, respectively.

a similar mass shift (M + 2) in the BOA adduct (Figs. 6*C* and 7*C*). As expected, incubations in the presence of $^{18}O_2$ and $H_2{}^{18}O$ yielded an [^{18}O]BOA adduct (*m/z* = 392.3387), which upon fragmentation resulted in loss of $H_2{}^{18}O$ (Figs. 6*D* and 7*D*). Parallel derivatization of the $^{16}O_2$ + $H_2{}^{16}O$ reaction products with DMG resulted in a predominant parent ion at *m/z* 370.3326 (Fig. 8*A*) as observed in Fig. 4*E*. Fragmentation of this ion yielded product ions corresponding to protonated DMG containing ^{16}O (*m/z* 104.0709) and a deformylated DMG fragment ion (*m/z* 58.0655) (Fig. 9*A*). For incubations containing either $^{18}O_2$ + $H_2{}^{16}O$ or $^{16}O_2$ + $H_2{}^{18}O$, a parent ion at *m/z* 372.3367 was observed, indicating incorporation of one ^{18}O atom into the DMG derivative (Fig. 8, *B* and *C*). Fragmentation of this ion (*m/z* = 372.3367) yielded ions at both *m/z* 104.0709 and *m/z* 106.0749 with the latter ion indicating the presence of ^{18}O in protonated DMG that was originally present in the hydroxyl group of the α-hydroxyaldehyde (Fig. 9, *B* and *C*). Importantly, incubations with both $^{18}O_2$ and $H_2{}^{18}O$ resulted in the expected M + 4 peak at *m/z* 374.3399, which was not observed from incubations with $^{18}O_2$ + $H_2{}^{16}O$ or $^{16}O_2$ + $H_2{}^{18}O$, indicating incorporation of two ^{18}O atoms from $^{18}O_2$ and $H_2{}^{18}O$ into the DMG adduct (Fig. 8*D*). Fragmentation of this molecular ion generated a predominant protonated DMG product ion at *m/z* 106.0750 (Fig. 9*D*). Remarkably, incubations with hydrogen [^{18}O]peroxide did not result in significant (<5%) incorporation of ^{18}O into the DMG derivative of the C18:0 α-hydroxyaldehyde (Fig. S4). We specifically point out that exchange of the aldo, keto, and *gem*-diol forms of the α-hydroxyaldehyde in water likely contributes to the observed distribution of the ^{18}O label present in the protonated DMG product ion. Mechanistically, these studies suggest that cyt *c* likely abstracts an electron from the stabilized resonance form of the vinyl ether bond to form a carbon-based radical that reacts with molecular oxygen to form a peroxy or epoxide intermediate (Fig. 10). Next, the positive charge on the vinyl ether oxygen is relieved by addition of H_2O to form a hemiacetal, which then spontaneously rearranges at neutral pH to yield the resultant α-hydroxyaldehyde and 2-acyl-lysolipid products.

Discussion

Despite nearly a century of investigation, the identity of the enzyme(s) responsible for the cleavage of the vinyl ether linkage in plasmenylcholine and plasmenylethanolamine has remained

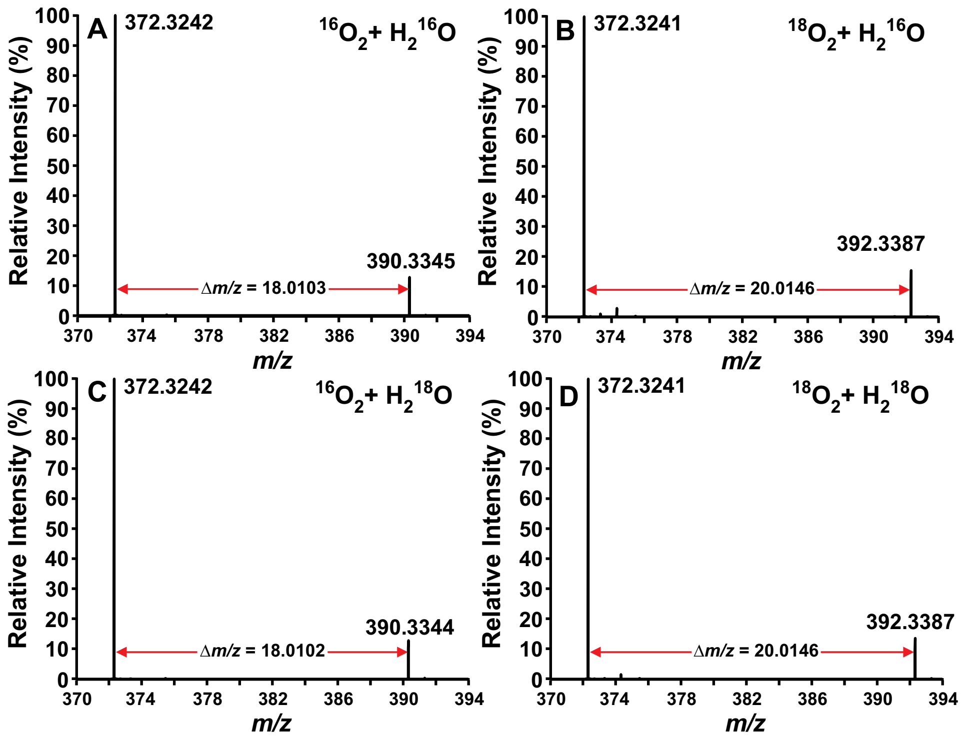

Figure 7. High-mass-accuracy MS^2 analysis of stable isotope–labeled BOA–α-hydroxyaldehyde derivatives. Plasmenyl-SAPC vesicles containing 10 mol % oxidized CL were incubated with cyt *c* in the presence of $^{16}O_2$ and $H_2^{16}O$ (*A*), $^{18}O_2$ and $H_2^{16}O$ (*B*), $^{16}O_2$ and $H_2^{18}O$ (*C*), or $^{18}O_2$ and $H_2^{18}O$ (*D*) for 30 min at 37 °C. Reaction products were extracted into cyclohexane/diethyl ether (4:1), derivatized with BOA, and analyzed by MS as described under "Experimental procedures." The mass of isotopic water (*i.e.* $\Delta m/z = 20.0146$) lost upon fragmentation of the ion at *m/z* 392.3387 (indicated between the *red arrows*) is indicative of the ^{18}O isotopic label present in the α-hydroxyl group of the C18:0 α-hydroxyaldehyde BOA derivative.

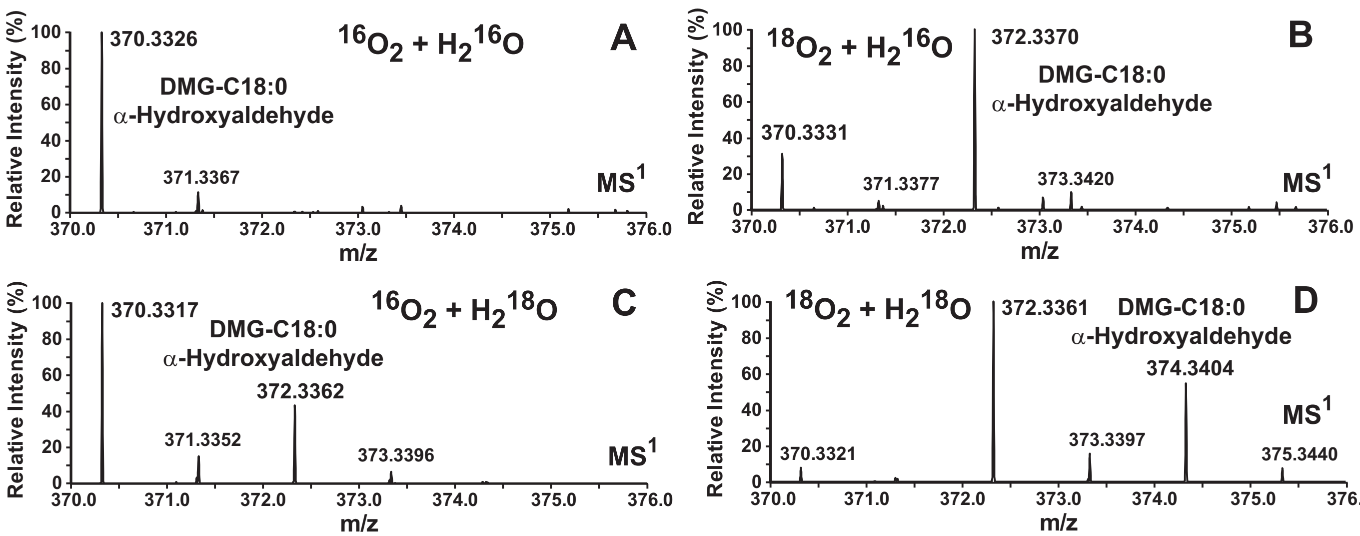

Figure 8. Incorporation of ^{18}O from $^{18}O_2$ and $H_2^{18}O$ into the DMG-derivatized α-hydroxyaldehyde product of the plasmalogenase reaction of cytochrome *c*. Plasmenyl-SAPC vesicles containing 10 mol % oxidized CL were incubated with cyt *c* in the presence of $^{16}O_2$ and $H_2^{16}O$ (*A*), $^{18}O_2$ and $H_2^{16}O$ (*B*), $^{16}O_2$ and $H_2^{18}O$ (*C*), or $^{18}O_2$ and $H_2^{18}O$ (*D*) for 30 min at 37 °C. Reaction products were extracted into cyclohexane/diethyl ether (4:1), derivatized with DMG, and analyzed by MS as described under "Experimental procedures." Peaks of DMG-derivatized C18:0 α-hydroxyaldehydes labeled with ^{16}O, ^{18}O, or two ^{18}O atoms are shown at *m/z* 370.3326, 372.3370, or 374.3404, respectively.

an enigma. Herein, we report the first molecular identification of a plasmalogenase in biology. The reaction mechanism is unique in that it utilizes the initial oxidation of the vinyl ether linkage by conformationally altered cyt *c* activating its cryptic peroxidase activity. Stable isotope experiments demonstrated that this leads to the addition of molecular oxygen to the α-carbon followed by the addition of water, yielding a hemiacetal intermediate that spontaneously rearranges at neutral pH to generate a 2-acyl-lysolipid and an α-hydroxyaldehyde (Fig. 10). Furthermore, the present study demonstrates that the vinyl ether linkage in plasmenylcholine and plasmenylethanolamine can be readily cleaved by cyt *c* in the presence of negatively charged phospholipids (*e.g.* tetra-18:2 CL, $PI(4,5)P_2$, or $PI(3,4,5)P_3$) and H_2O_2 or by oxidized CL alone.

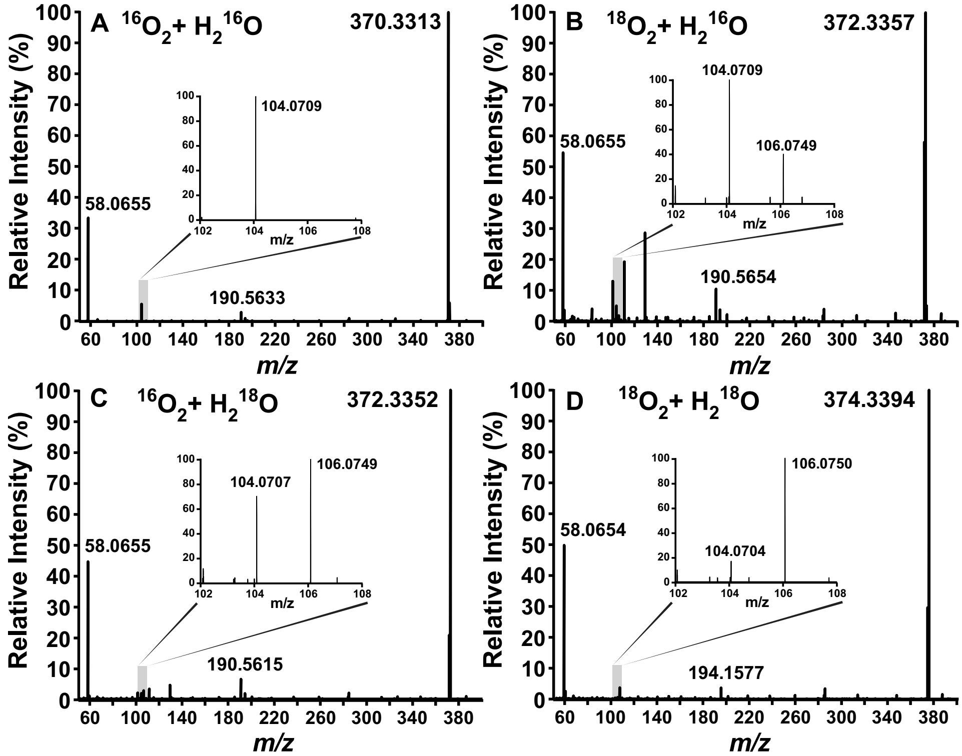

Figure 9. High-mass-accuracy MS^2 analysis of stable isotope–labeled DMG–α-hydroxyaldehyde derivatives. Plasmenyl-SAPC vesicles containing 10 mol % oxidized CL were incubated with cyt *c* in the presence of $^{16}O_2$ and $H_2{}^{16}O$ (*A*), $^{18}O_2$ and $H_2{}^{16}O$ (*B*), $^{16}O_2$ and $H_2{}^{18}O$ (*C*), or $^{18}O_2$ and $H_2{}^{18}O$ (*D*) for 30 min at 37 °C. Reaction products were extracted into cyclohexane/diethyl ether (4:1), derivatized with DMG, and analyzed by MS as described under "Experimental procedures."

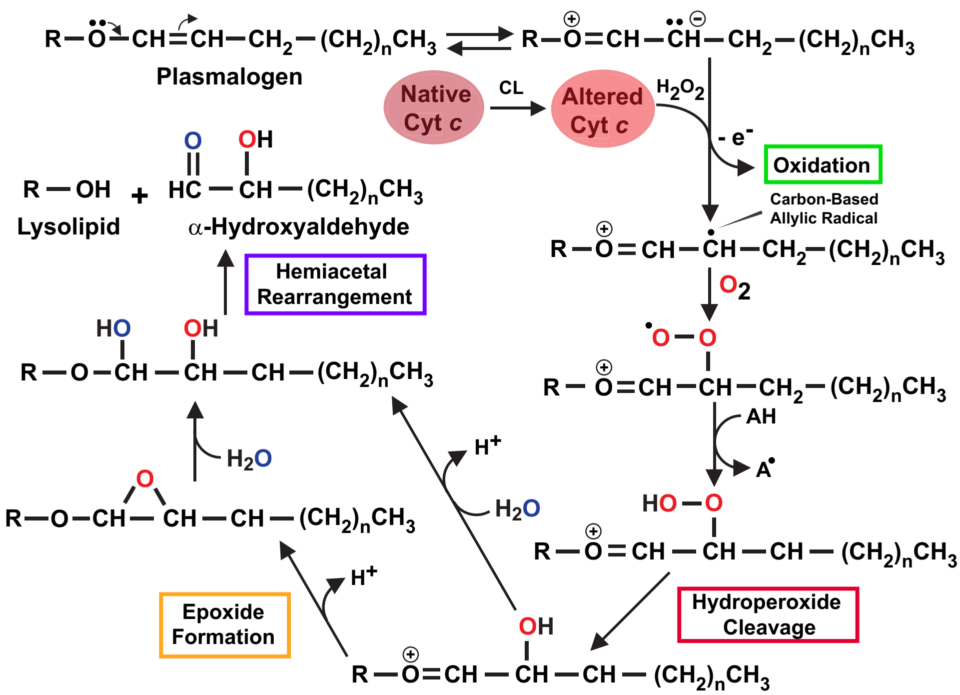

Figure 10. Proposed catalytic mechanism of the cytochrome *c* plasmalogenase reaction. The plasmalogen vinyl ether linkage exists as a resonance structure in which the oxygen can acquire a positive charge upon migration of an electron to the α-carbon. Cytochrome *c* extracts an electron from the α-carbon to form a carbon-based radical, which then readily reacts with molecular oxygen to form a peroxyl radical intermediate. After abstraction of a hydrogen radical (from any molecule (AH) that is a H$^{\cdot}$ donor) to form the hydroperoxide, this intermediate may then undergo either direct hydroperoxide cleavage to form a hydroxy intermediate or epoxidation to form an epoxide intermediate. Relief of the positive charge on the vinyl ether oxygen by water in both cases results in the formation of a common diol intermediate, which then undergoes a hemiacetal rearrangement to yield lysolipid and α-hydroxyaldehyde products. *R* = lysolipid backbone.

Previous studies have demonstrated the susceptibility of negatively charged lipids (*e.g.* CL and phosphatidylserine) to bind and induce conformational alterations that transform cyt *c* from an electron carrier to a potent peroxidase that can extract the bisallylic protons in CL (34, 38, 49). The resultant allylic radicals readily add molecular oxygen, resulting in the generation of CL hydroperoxides that can then be reduced to hydroxides (34). In contrast, incubations with zwitterionic diacyl PC and PE containing polyunsaturated fatty acyl chains were not effective in inducing cyt *c*–mediated oxidation in our hands and in agreement with previous studies (50). Our results demonstrate that cyt *c* is a highly active plasmalogenase after conformational alterations by negatively charged lipids that displace the axial Met-80, allowing access of H_2O_2 or organic peroxides (*e.g.* CL hydroperoxides) to activate its peroxidase activity, which is typical for many members of the peroxidase family of enzymes.

The present results demonstrate that ^{18}O from $^{18}O_2$ was predominantly incorporated into the hydroxyl group of the α-hydroxyaldehyde, whereas ^{18}O from $H_2{}^{18}O$ was delivered to the aldehyde carbon. This isotopic distribution indicates that the reaction sequence is likely initiated from a stable resonance form of vinyl ethers where an electron is transferred from the β-vinyl ether carbon (oxidation) to cyt *c* to form the allylic radical intermediate, which can then readily add molecular oxygen (Fig. 10). Next, the positive charge on the ether oxygen is relieved by addition of water to form the hemiacetal, which at neutral pH rearranges to form the lysolipid and the α-hydroxyaldehyde. It is also likely that after addition of molecular oxygen an epoxide can be formed, which then stereospecifically ring-opens to form the hemiacetal with subsequent rearrangement to the identified 2-acyl-lysolipid and α-hydroxyaldehyde reaction products (Fig. 10).

Typically, peroxidase activity results in incorporation of oxygen from H_2O_2 into the oxidized substrate. However, we could not observe any detectable incorporation of oxygen from $H_2{}^{18}O_2$ into the α-hydroxyaldehyde product. Thus, these stable isotope studies identify an unusual reaction coordinate where molecular oxygen is incorporated into the β-vinyl ether carbon whose hydrogen cannot be directly abstracted by a radical-mediated mechanism. Instead, a stable resonance form is utilized where an electron is extracted, effecting the oxidation of the vinyl ether linkage by interactions with activated cytochrome *c*. Moreover, it is unusual for peroxidases to directly incorporate molecular oxygen without the use of a radical intermediate ($OH^\bullet$ or $RO^\bullet$), which would lead to stable isotope scrambling.

Previously, a mammalian enzyme capable of hydrolytic cleavage of lysoplasmalogens through a nonoxidative mechanism has been identified (51). However, despite intense efforts to identify plasmalogen hydrolysis by this protein (Tmem86b, HUGO 28448), the results demonstrated that this enzyme does not possess plasmalogenase activity. Accordingly, Tmem86b plays a role in lysoplasmalogen catabolism in liver (51) likely with the obligatory participation of the lysoplasmalogen *sn*-2 hydroxy group through internal assistance that appears necessary for catalysis as originally proposed 50 years ago (52). In addition, leukocyte myeloperoxidase has been demonstrated to indirectly hydrolyze the vinyl ether linkage of plasmalogens through production of highly acidic HOCl or HOBr to generate α-haloaldehydes (53–57). Thus, the myeloperoxidase cleavage of plasmalogens is acid-catalyzed and is not mechanistically related to the oxidatively enabled hydrolytic cyt *c*–catalyzed plasmalogenase reaction described herein.

The demonstration of plasmenylcholine and plasmenylethanolamine in mitochondrial membranes suggests that cytochrome *c* can regulate/modulate multiple mitochondrial bioenergetic and signaling functions through its plasmalogenase activity. In addition, a substantial portion of myocardial mitochondria are in direct contact with the sarcoplasmic reticulum (SR) by tethering to mitofusin1 (58). Because the SR is highly enriched in plasmalogen molecular species (4) and tethered to mitochondria, the activation of cyt *c* plasmalogenase activity released from the mitochondrial intermembrane compartment in the immediate vicinity of the SR is anticipated to result in plasmalogen cleavage and alterations in SR calcium homeostasis. Furthermore, the existence of subsarcolemmal mitochondria in myocardium is well known (59). Accordingly, we propose that subsarcolemmal mitochondria can release cytochrome *c* in close spatial juxtaposition to the sarcolemmal membrane, which is highly enriched in plasmalogen molecular species containing AA (3), identifying numerous potential signaling functions. For example, lysolipids are known to precipitate alterations in electrophysiologic function, including ventricular tachyarrhythmias and sudden death (60), whereas arachidonic acid and its metabolites modulate ion channel kinetics (61, 62). Moreover, the highly reactive fatty acyl α-hydroxyaldehyde product is likely to covalently react with multiple nucleophiles to form adducts, which could be detrimental to the function of critical enzymes (63, 64). Finally, it is known that healthy cells can release small amounts of cyt *c* from mitochondria (65, 66), which we speculate could serve signaling functions between mitochondria and other intracellular organelles/membranes.

Recently, we have demonstrated that cyclooxygenase (COX)-2, but not COX-1, mediates the oxidation of 2-AA-LPC and 2-AA-LPE to generate specific eicosanoid lysolipids, which are potentially important signaling molecules (67). The previously unknown pathway identified in the current studies provides an alternative route to the generation of 2-AA-lysolipids for oxidation to biologically active signaling metabolites (Fig. 11). Alternatively, because plasmalogens are often highly enriched in AA, the hydrolysis of 2-AA–containing lysolipids by lysophospholipases can release arachidonic acid for multiple downstream metabolic and signaling pathways mediating proinflammatory and vasoactive effects among others (68–71).

In regard to ischemia/reperfusion, it is well established that the majority of cell death occurs in the center of the infarct zone with varying degrees of cell survival in the border zones. Recent studies have demonstrated that beneath a certain threshold level of damage to mitochondria, cardiac myocytes are able to remove these damaged mitochondria through mitophagy and survive (72). However, when the level of damage exceeds that which culling can adequately repair, cardiac myocyte death ensues. Thus, the salvage of cardiac myocytes in the border

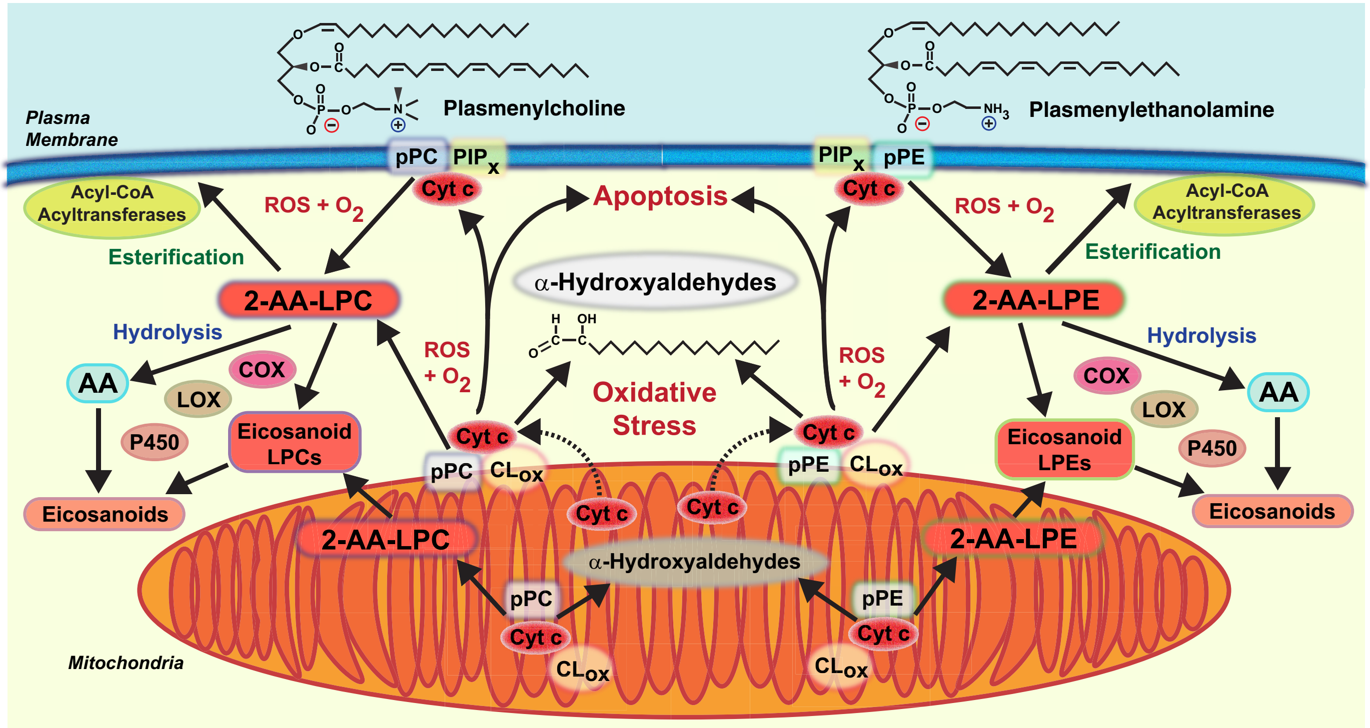

Figure 11. Lipid signaling pathways mediated by the plasmalogenase activity of cytochrome *c*. During oxidative stress, cytochrome *c* bound to negatively charged phospholipids (*e.g.* oxidized cardiolipin (CL_{ox})) undergoes a conformational change resulting in activation of its plasmalogenase activity and targeting of plasmalogens within mitochondria. Alternatively, outer membrane permeabilization of mitochondria during oxidative stress results in release of cytochrome *c* into the cytosol, leading to its association with negatively charged phospholipids in the mitochondria outer membrane (and associated membranes) or in other cellular membrane compartments (*e.g.* phosphatidylinositol phosphates (PIP_x) in the plasma membrane). The resultant 2-arachidonoyl-lysolipid and α-hydroxyaldehyde products of cyt *c* plasmalogenase activity serve as signaling molecules generated from plasmalogen-rich membranes. Furthermore, 2-arachidonoyl-lysolipids can either be esterified by acyl-CoA acyltransferases to diacyl phospholipids, metabolized by oxidases/oxygenases (*e.g.* COXs, lipoxygenases (*LOX*), or cytochromes P450 (*P450*)) to yield novel natural products or alternatively undergo hydrolysis (*e.g.* by lysophospholipases) to generate signaling eicosanoids. *ROS*, reactive oxygen species; *pPC*, plasmenylcholine; *pPE*, plasmenylethanolamine.

zone of an infarct is a primary goal of modern cardiology research. The present study identifies both a likely mechanism modulating mitochondrial communication and regulation of cardiac metabolism and signaling in normal myocardium as well as a potential therapeutic target for the salvage of damaged cardiac myocytes in border zones or in failing hearts. The potential implications of inhibiting this reaction to salvage myocardium to decrease morbidity and mortality have profound medical significance.

Previous studies have demonstrated a dramatic reduction (∼60% decrease) of plasmalogen molecular species in brains of patients with Alzheimer's disease (AD) (*e.g.* see Ref. 73). Furthermore, there have been numerous studies demonstrating that mitochondrial dysfunction precedes the deposition of amyloid and that mitochondrial oxidative stress or defective axonal transport is the proximal mediator of cognitive dysfunction in AD (*e.g.* see Refs. 74 and 75). Moreover, previous studies have identified the presence of α-hydroxyaldehydes in patients with AD, and the amount of α-hydroxyaldehydes was highly correlated with the state of cognitive dysfunction (76). Accordingly, we propose that cytochrome *c*–mediated degradation of plasmalogens due to increased oxidative stress is a potential mechanism responsible for the decrease in plasmalogens, membrane dysfunction, altered intramembrane proteolysis, and resultant cognitive abnormalities in patients with AD.

Collectively, the present study identifies conformationally activated cytochrome *c* as the first plasmalogenase in biology. Furthermore, cyt *c* initiates the cleavage of the vinyl ether bond in plasmalogens by a previously undescribed oxidatively enabled hydrolytic mechanism, generating a hemiacetal that spontaneously rearranges to produce 2-acyl-lysolipids and α-hydroxyaldehydes. This process has the catalytic potential to facilitate regulation of mitochondrial bioenergetics and signaling as well as communication with distal membrane compartments following release of cyt *c* from mitochondria during oxidative stress.

Experimental procedures

Materials

Equine cytochrome *c* (catalog number C7752) purified utilizing acetic acid according to the method of Hagihara *et al.* (77) and catalase (catalog number C40) from bovine liver (used without further purification) were obtained from Sigma-Aldrich. Recombinant bovine endothelial nitric-oxide synthase (catalog number 60880) was purchased from Cayman Chemical. 1-*O*-1′-(*Z*)-Octadecenyl-2-arachidonoyl-*sn*-glycero-3-phosphocholine (catalog number 852469C), 1-*O*-1′-(*Z*)-octadecenyl-2-arachidonoyl-*sn*-glycero-3-phosphoethanolamine (catalog number 852804C), 1-palmitoyl-2-arachidonoyl-*sn*-glycero-3-phosphocholine (catalog number 850459C), 1-palmitoyl-2-oleoyl-*sn*-glycero-3-phosphocholine (catalog number 850457C), bovine heart cardiolipin (∼95% tetra-18:2 cardiolipin) (catalog number 840012C), 1-stearoyl-

2-arachidonoyl-*sn*-glycero-3-phospho-(1′-*myo*-inositol-4′, 5′-bisphosphate) (catalog number 850165P), 1-stearoyl-2-arachidonoyl-*sn*-glycero-3-phospho-(1′-*myo*-inositol-3′,4′,5′-trisphosphate) (catalog number 850166P), 1,2-dimyristoleoyl-*sn*-glycero-3-phosphocholine (14:1 PC) (catalog number 850346P), 1-heptadecanoyl-2-hydroxy-*sn*-glycero-3-phosphocholine (17:0 LPC) (catalog number 855676P), 1,2-dipalmitoleoyl-*sn*-glycero-3-phosphoethanolamine (16:1 PE) (catalog number 850706P), 1-myristoyl-2-hydroxy-*sn*-glycero-3-phosphoethanolamine (14:0 LPE) (catalog number 856735P), and hexadecanal-d_9 (catalog number 857460 M) were purchased from Avanti Polar Lipids. Most other reagents were obtained from either Sigma-Aldrich or Fisher Scientific.

Preparation and purification of lipids

1-*O*-1′-(*Z*)-Octadecenyl-2-arachidonoyl-*sn*-glycero-3-phosphoethanolamine was purified prior to use utilizing an Ascentis C8 HPLC column (250 × 4.6 mm, 5 μm) using a linear gradient of solvent A (57% methanol, 23% acetonitrile, 20% 10 mM aqueous choline chloride) to solvent B (57% methanol, 43% acetonitrile) over 30 min. 2-AA-LPC and 2-AA-LPE were prepared by acid hydrolysis of 1-*O*-1′-(*Z*)-octadecenyl-2-arachidonoyl-*sn*-glycero-3-phosphocholine and 1-*O*-1′-(*Z*)-octadecenyl-2-arachidonoyl-*sn*-glycero-3-phosphoethanolamine, respectively, in methanol, 1 N sulfuric acid (95:5) at 70 °C (30 min) and subsequent HPLC purification (78, 79).

Chromatographic purification of cytochrome c

Equine cytochrome *c* was purchased from Sigma and further purified by FPLC utilizing a Mono S column equilibrated with 20 mM HEPES, pH 7.4, containing 0.1 mM DTPA. Briefly, 0.5 mg of solid equine cytochrome *c* was dissolved in 1 ml of 20 mM HEPES, pH 7.4, containing 0.1 mM DTPA and applied to a Mono S column equilibrated with the same buffer. Bound cytochrome *c* was eluted from the Mono S FPLC column using a linear gradient of NaCl (0–500 mM) over 25 column volumes. Fractions (0.5 ml) were collected and assayed for plasmalogenase activity using plasmenylcholine/CL SUVs in the presence of hydrogen peroxide as described below. Larger scale purifications of cytochrome *c* (50 mg) were performed utilizing an SP Sepharose column (1.5 × 15 cm) equilibrated with 20 mM HEPES, pH 7.4, containing 0.1 mM DTPA. Bound cytochrome *c* was eluted with a linear NaCl gradient (500 mM final concentration) over 12 column volumes (360 ml). Eluted cytochrome *c* was concentrated using Amicon centrifugal filter cartridges (3000 molecular weight cutoff). The concentration of cytochrome *c* was determined by the difference in absorbance between fully oxidized cytochrome *c* and reduced cytochrome *c* utilizing sodium dithionite (ϵ_{550} = 21.1 mM^{-1} cm^{-1}) (80). Absorbance determinations were made using a PerkinElmer Life Sciences LAMBDA 25 UV/visible double beam spectrophotometer with UV WinLab software.

Assay of plasmalogenase activity

For most reactions, 200 μl of purified cytochrome *c* (10 μM) in 10 mM potassium phosphate, pH 7.0, containing 0.25 mM DTPA was incubated with small unilamellar vesicles of plasmenyl-SAPC (250 μM) or plasmenyl-SAPE (125 μM)/POPC (125 μM) containing 10 mol % bovine heart cardiolipin (predominantly tetra-18:2 CL) with the indicated concentrations of hydrogen peroxide for 10 min at 37 °C. The concentration of hydrogen peroxide was measured using an extinction coefficient, ϵ_{240}, of 43.6 M^{-1} cm^{-1}. For some reactions, cardiolipin preoxidized by cytochrome *c* and H_2O_2 or phosphatidylinositol phosphates ($PI(4,5)P_2$ and $PI(3,4,5)P_3$) were substituted for nonoxidized cardiolipin. Reactions were terminated by addition of 1 ml of methanol, the samples were placed on ice, and 1 ml of chloroform was added. Next, appropriate internal standards (5 nmol of 17:0 LPC and 50 nmol of 14:1 PC for reactions with plasmenylcholine and 5 nmol of 14:0 LPE and 50 nmol of 16:1 PE for reactions with plasmenylethanolamine) were added. Phase separation was induced by addition of 900 μl of 25 mM NaCl followed by vigorous vortexing and centrifugation to effect phase partitioning. The water-methanol layer was re-extracted with chloroform and combined with the original chloroform layer from the first extraction, and samples were dried under a nitrogen stream.

Mass spectrometric identification and quantitation of 2-acyl-lysophospholipids

Mass spectrometric analysis was performed using a TSQ Quantum Ultra mass spectrometer (Thermo Fisher Scientific, San Jose, CA) equipped with an automated nanospray apparatus (Nanomate HD, Advion BioSciences, Ithaca, NY) for direct infusion MS as described previously (81). The capillary temperature of the mass spectrometer was set at 150 °C. The spray voltage and gas pressure of the Nanomate were set at 1.3 kV and 1.1 p.s.i., respectively. Mass spectrometric analyses including full-mass MS^1 spectra and tandem mass spectrometric analyses were all performed in the positive-ion mode. Identification of 2-AA-LPC and 2-AA-LPE was performed by ESI-MS and/or ESI-MS/MS mass spectrometric analyses of the sodiated molecular ion at *m/z* 566 for 2-AA-LPC, the protonated molecular ion at *m/z* 502 for 2-AA-LPE, or the sodiated molecular ion at *m/z* 524 for 2-AA-LPE. The regiospecificity of AA-LPC and AA-LPE was determined by the ratio of product ions as described previously (46, 71). The sodiated 2-AA-LPC and 2-AA-LPE were also analyzed using a hybrid mass spectrometer (LTQ-Orbitrap, Thermo Fisher Scientific) by direct infusion in the positive-ion mode with sheath, auxiliary, and sweep gas flows of 4, 1, and 0 arbitrary units, respectively. The capillary temperature was set at 275 °C, the electrospray voltage was 4.0 kV, and tube lens were set to 100 V. The instrument was calibrated as instructed by the manufacturer prior to use. The isolation width was set to ±1 thomson, normalized collision energy was set at 30 eV for 2-AA-LPC and 22 eV for 2-AA-LPE, and resolution was 30,000 at *m/z* 400. Instrument control and data acquisition were performed using Thermo Xcalibur version 2.1 software.

Derivatization and mass spectrometric identification of α-hydroxy fatty aldehydes

Reaction products from incubations of plasmenyl-SAPC SUVs containing 10 mol % bovine heart CL in the presence or absence of cyt *c* and H_2O_2 were extracted into an equal volume of cyclohexane/diethyl ether (4:1). α-Hydroxy fatty aldehydes were derivatized with DMG in a new tube by a modified procedure (48) in the presence of hexadecanol (1 nmol) and analyzed in the positive-ion mode. Briefly, to the dried cyclohexane/diethyl ether extract, 5 μl of a mixture of *N*,*N*-dimethylglycine HCl (1 M) and DMAP (1 M) were added in anhydrous chloroform followed by addition of 10 μl of *N*-(3-dimethylaminopropyl)-*N*′-ethylcarbodiimide hydrochloride (0.25 M) in anhydrous chloroform, 200 μl of anhydrous chloroform, and 100 mg of 4-Å molecular sieve followed by vortexing and incubation at 45 °C for 60 min. Reactions were stopped by drying the solvent under an N_2 stream followed by resuspension in 200 μl of isopropyl alcohol and analysis by LC-MS/MS as described below. α-Hydroxyaldehydes were also derivatized with BOA in the presence of 1 ml of 0.1 M borax buffer, pH 9.4, containing 1 nmol of fatty aldehyde internal standard (hexadecanal-d_9) as described previously (47). Briefly, 2 μmol of BOA was added to each reaction in borax buffer and incubated for 3 h at room temperature. An equal volume of cyclohexane/diethyl ether (4:1, v/v) was then added with vortexing and centrifuged to separate organic and aqueous layers. The upper organic layer was transferred to a new tube, 1 ml of cyclohexane/diethyl ether was added to the remaining aqueous phase, and the mixture was vortexed and subsequently centrifuged to separate the layers. The organic phases were combined and dried under a nitrogen stream prior to mass spectral analysis.

The BOA- and DMG-derivatized α-hydroxyaldehydes were analyzed by LC-MS/MS using a Surveyor HPLC system and an LTQ-Orbitrap mass spectrometer. The BOA- or DMG-derivatized α-hydroxyaldehydes were separated with a C18 reverse-phase column (Kinetics EVO C18, 5 μm, 150 × 2.1 mm) at 22 °C with a flow rate of 200 μl/min. A linear gradient of solvent A (water with 10 mM ammonium acetate, pH 4.3) and solvent B (isopropyl alcohol) was used as follows: 0 min, 25% B; 5 min, 25% B; 20 min, 100% B; 25 min, 100% B; 25.1 min, 25% B; 30 min, 25% B. The sample injection volume was 10 μl, and the autosampler tray temperature was set at 4 °C. The spray voltage in the ESI source was 4.1 kV. The sheath gas flow rate was 40. The capillary temperature was 270 °C. The BOA- and DMG-derivatized α-hydroxyaldehydes were also analyzed by tandem MS. The collision energy used was 30 eV (collision-induced dissociation) for the BOA-derivatized sample and 35 eV (high-energy collision dissociation) for the DMG-derivatized sample with an isolation width of ±1.5 thomsons.

Measurement of incorporation of ^{18}O from $^{18}O_2$ and $H_2{}^{18}O$ into plasmalogenase reaction products

Plasmenyl-SAPC vesicles containing 10 mol % cardiolipin in 10 mM potassium phosphate buffer, pH 7.0, containing 0.25 mM DTPA was 1) purged with $^{18}O_2$ (97% ^{18}O atom enrichment) in a sealed 1-ml vial with a septum, 2) incubated with $H_2{}^{18}O$ (97% ^{18}O atom enrichment), or 3) incubated with $H_2{}^{18}O_2$ (500 μM final concentration, 90% ^{18}O atom enrichment). Concentrated cytochrome *c* (1 mM) was then injected into the vial to 10 μM final concentration and vortexed. After incubation for 30 min at 37 °C, the reaction was terminated by addition of 0.8 ml of cyclohexane/diethyl ether (4:1) and vortexed. The upper organic layer was removed, and the remaining aqueous layer was re-extracted with 0.8 ml of cyclohexane/diethyl ether (4:1). The combined organic layers were then dried under a nitrogen stream and subjected to derivatization and LC-MS/MS analysis as described above.

Isolation of rabbit heart mitochondria, induction of mPTP opening, and release of cytochrome c

Male New Zealand rabbits were sedated with ketamine/xylazine (35/5 mg/kg) prior to euthanasia with pentobarbital (150 mg/kg) and removal of the heart under a protocol approved by the Washington University Animal Studies committee. After thorough washing with PBS to remove excess blood, the heart was finely diced with a razor blade prior to homogenization using a Teflon homogenizer (150 rpm × 10 passes) in mitochondrial isolation buffer (MIB) (10 mM HEPES, pH 7.4, containing 0.21 M mannitol and 0.07 M sucrose) containing 5 mg/ml fatty acid–free BSA. Following pelleting of myofibrils/nuclei/cell debris by low speed centrifugation (1000 × *g* for 7 min), mitochondria were isolated from the resultant supernatant by differential centrifugation at 10,000 × *g* for 10 min. Mitochondria were washed three times with MIB without BSA before use. Release of cyt *c* was induced by incubation of mitochondria in MIB containing 75 mM KCl and 75 μM $CaHPO_4$ for 35 °C for 30 min. Swollen mitochondria were then pelleted by centrifugation at 10,000 × *g* for 10 min to obtain the supernatant fraction. Proteins in the resultant supernatant and remaining mitochondria (pelleted by centrifugation) were resolved by SDS-PAGE (14% gel), transferred to PVDF membranes, and probed for cytochrome *c* content by ECL Western blot analysis utilizing a monoclonal cyt *c* antibody and anti-mouse IgG-HRP conjugate as described previously (83). The supernatant was analyzed for plasmalogenase activity using CL oxidized by cyt *c* in the absence or presence of a mAb (1 μg) directed against cyt *c* as described above.

Collection of human heart tissue and isolation of mitochondria

Human heart tissue was obtained from Mid-America Transplant (St. Louis, MO) and the Washington University Translational Cardiovascular Tissue Core. Tissue from the left ventricle and left ventricular apex of nonfailing human hearts was obtained from organ donors having a heart deemed unsuitable for transplantation due to donor age, epicardial (nonocclusive) coronary vascular disease, or high risk behavioral profile. All tissue was trimmed of excess fat, washed in cold PBS, and then placed in ice-cold MIB prior to isolation of mitochondria by differential centrifugation as described previously (84).

Determination of plasmenyl-PC and plasmenyl-PE content of human heart mitochondrial phospholipids by shotgun lipidomics

Isolated human heart mitochondria were extracted into chloroform using a Bligh-Dyer extraction method in the presence of internal standards (14:1 PC and 16:1 PE) as described previously (85). Phosphatidylethanolamine phospholipids were derivatized with fluorenylmethoxycarbonyl (Fmoc) chloride as described previously (86). Acid hydrolysis of plasmalogens was performed as described above, cleaving only vinyl ether lipids without affecting either diacyl or alkyl ether phospholipids. The resultant lipid extracts were analyzed utilizing a TSQ Quantum Ultra Plus triple-quadrupole mass spectrometer as described above.

Binding of cyt c to LUVs

LUVs were prepared by extrusion of 1-*O*-1′-(*Z*)-octadecenyl-2-arachidonoyl-*sn*-glycero-3-phosphocholine (1.25 mM) with or without nonoxidized CL (10 mol %) or previously oxidized CL (10 mol %) in 10 mM potassium phosphate buffer, pH 7.0, containing 0.25 mM DTPA and 48 mM sucrose through a 0.8-μm filter. LUVs (0.2 ml) were diluted 1:5 in 10 mM potassium phosphate, pH 7.0, containing 0.25 mM DTPA and 25 mM KCl prior to addition of purified cyt *c* (2.5 μM final concentration). Following incubation for 5 min at room temperature, the samples were then centrifuged at 100,000 × *g* at 15 °C for 1 h. The supernatants were removed, and the pelleted LUVs were resuspended in 0.5 ml of buffer prior to analysis of cyt *c* content by SDS-PAGE and immunoblot analysis as described above.

Oxidation of cardiolipin by cytochrome c and hydrogen peroxide

Bovine heart cardiolipin was oxidized by cyt *c* as described previously (87) with minor modifications. Briefly, CL SUVs (250 μM) in 10 mM potassium phosphate buffer, pH 7.0, containing 0.25 mM DTPA were incubated with cyt *c* and hydrogen peroxide at 37 °C for 40 min. Cytochrome *c* (10 nmol) and H_2O_2 (50 nmol) were added at 10-min intervals to achieve 50 and 250 μM final concentrations, respectively, at the end of the incubation. Following addition of KCl to 100 mM, oxidized CL was extracted into chloroform following the Folch extraction method (82).

Author contributions—C. M. J. and R. W. G. conceptualization; C. M. J., K. Y., and R. W. G. supervision; C. M. J. and R. W. G. funding acquisition; C. M. J., K. Y., G. L., S. H. M., and B. G. D. investigation; C. M. J., K. Y., G. L., and S. H. M. visualization; C. M. J., K. Y., G. L., and R. W. G. methodology; C. M. J., K. Y., and R. W. G. writing-original draft; C. M. J., K. Y., G. L., S. H. M., and R. W. G. writing-review and editing.

References

1. Feulgen, R., and Voit, K. (1924) A widely-dispersing compact aldehyde. Its development at a preliminary stage, its microchemical and microscopic-chemical evidence and the means to its preparative representation. *Pflugers Arch. Gesamte Physiol. Menschen Tiere* **206,** 389–410 CrossRef
2. Rapport, M. M., Lerner, B., Alonzo, N., and Franzl, R. E. (1957) The structure of plasmalogens. II. Crystalline lysophosphatidal ethanolamine (acetal phospholipide). *J. Biol. Chem.* **225,** 859–867 Medline
3. Gross, R. W. (1984) High plasmalogen and arachidonic acid content of canine myocardial sarcolemma: a fast atom bombardment mass spectroscopic and gas chromatography-mass spectroscopic characterization. *Biochemistry* **23,** 158–165 CrossRef Medline
4. Gross, R. W. (1985) Identification of plasmalogen as the major phospholipid constituent of cardiac sarcoplasmic reticulum. *Biochemistry* **24,** 1662–1668 CrossRef Medline
5. Brites, P., Waterham, H. R., and Wanders, R. J. (2004) Functions and biosynthesis of plasmalogens in health and disease. *Biochim. Biophys. Acta* **1636,** 219–231 CrossRef Medline
6. Wallner, S., and Schmitz, G. (2011) Plasmalogens the neglected regulatory and scavenging lipid species. *Chem. Phys. Lipids* **164,** 573–589 CrossRef Medline
7. Braverman, N. E., and Moser, A. B. (2012) Functions of plasmalogen lipids in health and disease. *Biochim. Biophys. Acta* **1822,** 1442–1452 CrossRef Medline
8. Ford, D. A., and Gross, R. W. (1989) Plasmenylethanolamine is the major storage depot for arachidonic acid in rabbit vascular smooth muscle and is rapidly hydrolyzed after angiotensin II stimulation. *Proc. Natl. Acad. Sci. U.S.A.* **86,** 3479–3483 CrossRef Medline
9. Hazen, S. L., Ford, D. A., and Gross, R. W. (1991) Activation of a membrane-associated phospholipase A_2 during rabbit myocardial ischemia which is highly selective for plasmalogen substrate. *J. Biol. Chem.* **266,** 5629–5633 Medline
10. Yoda, E., Rai, K., Ogawa, M., Takakura, Y., Kuwata, H., Suzuki, H., Nakatani, Y., Murakami, M., and Hara, S. (2014) Group VIB calcium-independent phospholipase A_2 (iPLA$_2\gamma$) regulates platelet activation, hemostasis and thrombosis in mice. *PLoS One* **9,** e109409 CrossRef Medline
11. Albi, E., Cataldi, S., Magni, M. V., and Sartori, C. (2004) Plasmalogens in rat liver chromatin: new molecules involved in cell proliferation. *J. Cell. Physiol.* **201,** 439–446 CrossRef Medline
12. Munn, N. J., Arnio, E., Liu, D., Zoeller, R. A., and Liscum, L. (2003) Deficiency in ethanolamine plasmalogen leads to altered cholesterol transport. *J. Lipid Res.* **44,** 182–192 CrossRef Medline
13. Stadelmann-Ingrand, S., Favreliere, S., Fauconneau, B., Mauco, G., and Tallineau, C. (2001) Plasmalogen degradation by oxidative stress: production and disappearance of specific fatty aldehydes and fatty α-hydroxyaldehydes. *Free Radic. Biol. Med.* **31,** 1263–1271 CrossRef Medline
14. Engelmann, B. (2004) Plasmalogens: targets for oxidants and major lipophilic antioxidants. *Biochem. Soc. Trans.* **32,** 147–150 CrossRef Medline
15. Waterham, H. R., Ferdinandusse, S., and Wanders, R. J. (2016) Human disorders of peroxisome metabolism and biogenesis. *Biochim. Biophys. Acta* **1863,** 922–933 CrossRef Medline
16. Honsho, M., and Fujiki, Y. (2017) Plasmalogen homeostasis—regulation of plasmalogen biosynthesis and its physiological consequence in mammals. *FEBS Lett.* **591,** 2720–2729 CrossRef Medline
17. Dorninger, F., Forss-Petter, S., and Berger, J. (2017) From peroxisomal disorders to common neurodegenerative diseases—the role of ether phospholipids in the nervous system. *FEBS Lett.* **591,** 2761–2788 CrossRef Medline
18. Shah, M. S., and Brownlee, M. (2016) Molecular and cellular mechanisms of cardiovascular disorders in diabetes. *Circ. Res.* **118,** 1808–1829 CrossRef Medline
19. Lejay, A., Fang, F., John, R., Van, J. A., Barr, M., Thaveau, F., Chakfe, N., Geny, B., and Scholey, J. W. (2016) Ischemia reperfusion injury, ischemic conditioning and diabetes mellitus. *J. Mol. Cell. Cardiol.* **91,** 11–22 CrossRef Medline
20. Kayama, Y., Raaz, U., Jagger, A., Adam, M., Schellinger, I. N., Sakamoto, M., Suzuki, H., Toyama, K., Spin, J. M., and Tsao, P. S. (2015) Diabetic cardiovascular disease induced by oxidative stress. *Int. J. Mol. Sci.* **16,** 25234–25263 CrossRef Medline
21. Kayar, S. R., and Banchero, N. (1987) Volume density and distribution of mitochondria in myocardial growth and hypertrophy. *Respir. Physiol.* **70,** 275–286 Medline
22. Chen, Y. R., and Zweier, J. L. (2014) Cardiac mitochondria and reactive oxygen species generation. *Circ. Res.* **114,** 524–537 CrossRef Medline
23. Borutaite, V., Toleikis, A., and Brown, G. C. (2013) In the eye of the storm: mitochondrial damage during heart and brain ischaemia. *FEBS J.* **280,** 4999–5014 CrossRef Medline
24. Ong, S. B., and Gustafsson, A. B. (2012) New roles for mitochondria in cell death in the reperfused myocardium. *Cardiovasc. Res.* **94,** 190–196 CrossRef Medline
25. Hüttemann, M., Helling, S., Sanderson, T. H., Sinkler, C., Samavati, L., Mahapatra, G., Varughese, A., Lu, G., Liu, J., Ramzan, R., Vogt, S., Grossman, L. I., Doan, J. W., Marcus, K., and Lee, I. (2012) Regulation of mitochondrial respiration and apoptosis through cell signaling: cytochrome *c* oxidase and cytochrome *c* in ischemia/reperfusion injury and inflammation. *Biochim. Biophys. Acta* **1817,** 598–609 CrossRef Medline

26. Pasdois, P., Parker, J. E., Griffiths, E. J., and Halestrap, A. P. (2011) The role of oxidized cytochrome *c* in regulating mitochondrial reactive oxygen species production and its perturbation in ischaemia. *Biochem. J.* **436,** 493–505 CrossRef Medline
27. Kadenbach, B., Ramzan, R., Moosdorf, R., and Vogt, S. (2011) The role of mitochondrial membrane potential in ischemic heart failure. *Mitochondrion* **11,** 700–706 CrossRef Medline
28. Honda, H. M., Korge, P., and Weiss, J. N. (2005) Mitochondria and ischemia/reperfusion injury. *Ann. N.Y. Acad. Sci.* **1047,** 248–258 CrossRef Medline
29. Santucci, R., Sinibaldi, F., Polticelli, F., and Fiorucci, L. (2014) Role of cardiolipin in mitochondrial diseases and apoptosis. *Curr. Med. Chem.* **21,** 2702–2714 CrossRef Medline
30. Kilbride, S. M., and Prehn, J. H. (2013) Central roles of apoptotic proteins in mitochondrial function. *Oncogene* **32,** 2703–2711 CrossRef Medline
31. Tait, S. W., and Green, D. R. (2010) Mitochondria and cell death: outer membrane permeabilization and beyond. *Nat. Rev. Mol. Cell Biol.* **11,** 621–632 CrossRef Medline
32. Kapralov, A. A., Kurnikov, I. V., Vlasova, I. I., Belikova, N. A., Tyurin, V. A., Basova, L. V., Zhao, Q., Tyurina, Y. Y., Jiang, J., Bayir, H., Vladimirov, Y. A., and Kagan, V. E. (2007) The hierarchy of structural transitions induced in cytochrome *c* by anionic phospholipids determines its peroxidase activation and selective peroxidation during apoptosis in cells. *Biochemistry* **46,** 14232–14244 CrossRef Medline
33. Ascenzi, P., Polticelli, F., Marino, M., Santucci, R., and Coletta, M. (2011) Cardiolipin drives cytochrome *c* proapoptotic and antiapoptotic actions. *IUBMB Life* **63,** 160–165 CrossRef Medline
34. Kagan, V. E., Tyurin, V. A., Jiang, J., Tyurina, Y. Y., Ritov, V. B., Amoscato, A. A., Osipov, A. N., Belikova, N. A., Kapralov, A. A., Kini, V., Vlasova, I. I., Zhao, Q., Zou, M., Di, P., Svistunenko, D. A., *et al*. (2005) Cytochrome *c* acts as a cardiolipin oxygenase required for release of proapoptotic factors. *Nat. Chem. Biol.* **1,** 223–232 CrossRef Medline
35. Tyurina, Y. Y., Poloyac, S. M., Tyurin, V. A., Kapralov, A. A., Jiang, J., Anthonymuthu, T. S., Kapralova, V. I., Vikulina, A. S., Jung, M. Y., Epperly, M. W., Mohammadyani, D., Klein-Seetharaman, J., Jackson, T. C., Kochanek, P. M., Pitt, B. R., *et al.* (2014) A mitochondrial pathway for biosynthesis of lipid mediators. *Nat. Chem.* **6,** 542–552 CrossRef Medline
36. Liu, G. Y., Moon, S. H., Jenkins, C. M., Li, M., Sims, H. F., Guan, S., and Gross, R. W. (2017) The phospholipase iPLA$_2\gamma$ is a major mediator releasing oxidized aliphatic chains from cardiolipin integrating mitochondrial bioenergetics and signaling. *J. Biol. Chem.* **292,** 10672–10684 CrossRef Medline
37. Scherrer, L. A., and Gross, R. W. (1989) Subcellular distribution, molecular dynamics and catabolism of plasmalogens in myocardium. *Mol. Cell. Biochem.* **88,** 97–105 Medline
38. Iwase, H., Takatori, T., Nagao, M., Iwadate, K., and Nakajima, M. (1996) Monoepoxide production from linoleic acid by cytochrome *c* in the presence of cardiolipin. *Biochem. Biophys. Res. Commun.* **222,** 83–89 CrossRef Medline
39. Ascenzi, P., Coletta, M., Wilson, M. T., Fiorucci, L., Marino, M., Polticelli, F., Sinibaldi, F., and Santucci, R. (2015) Cardiolipin-cytochrome *c* complex: switching cytochrome *c* from an electron-transfer shuttle to a myoglobin- and a peroxidase-like heme-protein. *IUBMB Life* **67,** 98–109 CrossRef Medline
40. Basova, L. V., Kurnikov, I. V., Wang, L., Ritov, V. B., Belikova, N. A., Vlasova, I. I., Pacheco, A. A., Winnica, D. E., Peterson, J., Bayir, H., Waldeck, D. H., and Kagan, V. E. (2007) Cardiolipin switch in mitochondria: shutting off the reduction of cytochrome *c* and turning on the peroxidase activity. *Biochemistry* **46,** 3423–3434 CrossRef Medline
41. Bayir, H., Fadeel, B., Palladino, M. J., Witasp, E., Kurnikov, I. V., Tyurina, Y. Y., Tyurin, V. A., Amoscato, A. A., Jiang, J., Kochanek, P. M., DeKosky, S. T., Greenberger, J. S., Shvedova, A. A., and Kagan, V. E. (2006) Apoptotic interactions of cytochrome *c*: redox flirting with anionic phospholipids within and outside of mitochondria. *Biochim. Biophys. Acta* **1757,** 648–659 CrossRef Medline
42. Belikova, N. A., Tyurina, Y. Y., Borisenko, G., Tyurin, V., Samhan Arias, A. K., Yanamala, N., Furtmüller, P. G., Klein-Seetharaman, J., Obinger, C., and Kagan, V. E. (2009) Heterolytic reduction of fatty acid hydroperoxides by cytochrome *c*/cardiolipin complexes: antioxidant function in mitochondria. *J. Am. Chem. Soc.* **131,** 11288–11289 CrossRef Medline
43. Cadenas, E., Boveris, A., and Chance, B. (1980) Low-level chemiluminescence of hydroperoxide-supplemented cytochrome *c*. *Biochem. J.* **187,** 131–140 CrossRef Medline
44. Kim, N. H., and Kang, J. H. (2006) Oxidative damage of DNA induced by the cytochrome c and hydrogen peroxide system. *J. Biochem. Mol. Biol.* **39,** 452–456 Medline
45. Bakan, A., Kapralov, A. A., Bayir, H., Hu, F., Kagan, V. E., and Bahar, I. (2015) Inhibition of peroxidase activity of cytochrome *c*: *de novo* compound discovery and validation. *Mol. Pharmacol.* **88,** 421–427 CrossRef Medline
46. Han, X. L., and Gross, R. W. (1996) Structural determination of lysophospholipid regioisomers by electrospray ionization tandem mass spectrometry. *J. Am. Chem. Soc.* **118,** 451–457 CrossRef
47. Jain, V., and Thielen, D. (1995) Determination of aldehydes in basic medium by gas chromatography using O-benzylhydroxylamine derivatization. *J. Chromatogr. A* **709,** 387–392 CrossRef
48. Wang, M., Hayakawa, J., Yang, K., and Han, X. (2014) Characterization and quantification of diacylglycerol species in biological extracts after one-step derivatization: a shotgun lipidomics approach. *Anal. Chem.* **86,** 2146–2155 CrossRef Medline
49. Kagan, V. E., Borisenko, G. G., Tyurina, Y. Y., Tyurin, V. A., Jiang, J., Potapovich, A. I., Kini, V., Amoscato, A. A., and Fujii, Y. (2004) Oxidative lipidomics of apoptosis: redox catalytic interactions of cytochrome *c* with cardiolipin and phosphatidylserine. *Free Radic. Biol. Med.* **37,** 1963–1985 CrossRef Medline
50. Tyurin, V. A., Tyurina, Y. Y., Feng, W., Mnuskin, A., Jiang, J., Tang, M., Zhang, X., Zhao, Q., Kochanek, P. M., Clark, R. S., Bayir, H., and Kagan, V. E. (2008) Mass-spectrometric characterization of phospholipids and their primary peroxidation products in rat cortical neurons during staurosporine-induced apoptosis. *J. Neurochem.* **107,** 1614–1633 CrossRef Medline
51. Wu, L. C., Pfeiffer, D. R., Calhoon, E. A., Madiai, F., Marcucci, G., Liu, S., and Jurkowitz, M. S. (2011) Purification, identification, and cloning of lysoplasmalogenase, the enzyme that catalyzes hydrolysis of the vinyl ether bond of lysoplasmalogen. *J. Biol. Chem.* **286,** 24916–24930 CrossRef Medline
52. Warner, H. R., and Lands, W. E. (1961) The metabolism of plasmalogen: enzymatic hydrolysis of the vinyl ether. *J. Biol. Chem.* **236,** 2404–2409 Medline
53. Albert, C. J., Crowley, J. R., Hsu, F. F., Thukkani, A. K., and Ford, D. A. (2001) Reactive chlorinating species produced by myeloperoxidase target the vinyl ether bond of plasmalogens: identification of 2-chlorohexadecanal. *J. Biol. Chem.* **276,** 23733–23741 CrossRef Medline
54. Albert, C. J., Crowley, J. R., Hsu, F. F., Thukkani, A. K., and Ford, D. A. (2002) Reactive brominating species produced by myeloperoxidase target the vinyl ether bond of plasmalogens: disparate utilization of sodium halides in the production of α-halo fatty aldehydes. *J. Biol. Chem.* **277,** 4694–4703 CrossRef Medline
55. Thukkani, A. K., Hsu, F. F., Crowley, J. R., Wysolmerski, R. B., Albert, C. J., and Ford, D. A. (2002) Reactive chlorinating species produced during neutrophil activation target tissue plasmalogens: production of the chemoattractant, 2-chlorohexadecanal. *J. Biol. Chem.* **277,** 3842–3849 CrossRef Medline
56. Thukkani, A. K., Albert, C. J., Wildsmith, K. R., Messner, M. C., Martinson, B. D., Hsu, F. F., and Ford, D. A. (2003) Myeloperoxidase-derived reactive chlorinating species from human monocytes target plasmalogens in low density lipoprotein. *J. Biol. Chem.* **278,** 36365–36372 CrossRef Medline
57. Albert, C. J., Thukkani, A. K., Heuertz, R. M., Slungaard, A., Hazen, S. L., and Ford, D. A. (2003) Eosinophil peroxidase-derived reactive brominating species target the vinyl ether bond of plasmalogens generating a novel chemoattractant, α-bromo fatty aldehyde. *J. Biol. Chem.* **278,** 8942–8950 CrossRef Medline
58. Hall, A. R., Burke, N., Dongworth, R. K., Kalkhoran, S. B., Dyson, A., Vicencio, J. M., Dorn, G. W., II, Yellon, D. M., and Hausenloy, D. J. (2016) Hearts deficient in both Mfn1 and Mfn2 are protected against acute myocardial infarction. *Cell Death Dis.* **7,** e2238 CrossRef Medline

59. Palmer, J. W., Tandler, B., and Hoppel, C. L. (1986) Heterogeneous response of subsarcolemmal heart mitochondria to calcium. *Am. J. Physiol. Heart Circ. Physiol.* **250,** H741–H748 Medline
60. Gross, R. W., Corr, P. B., Lee, B. I., Saffitz, J. E., Crafford, W. A., Jr, and Sobel, B. E. (1982) Incorporation of radiolabeled lysophosphatidyl choline into canine Purkinje fibers and ventricular muscle. Electrophysiological, biochemical, and autoradiographic correlations. *Circ. Res.* **51,** 27–36 CrossRef Medline
61. Chemin, J., Cazade, M., and Lory, P. (2014) Modulation of T-type calcium channels by bioactive lipids. *Pflugers Arch.* **466,** 689–700 CrossRef Medline
62. Spector, A. A., and Kim, H. Y. (2015) Cytochrome P450 epoxygenase pathway of polyunsaturated fatty acid metabolism. *Biochim. Biophys. Acta* **1851,** 356–365 CrossRef Medline
63. Sayre, L. M., Lin, D., Yuan, Q., Zhu, X., and Tang, X. (2006) Protein adducts generated from products of lipid oxidation: focus on HNE and one. *Drug Metab. Rev.* **38,** 651–675 CrossRef Medline
64. Domingues, R. M., Domingues, P., Melo, T., Pérez-Sala, D., Reis, A., and Spickett, C. M. (2013) Lipoxidation adducts with peptides and proteins: deleterious modifications or signaling mechanisms? *J. Proteomics* **92,** 110–131 CrossRef Medline
65. Von Ahsen, O., Waterhouse, N. J., Kuwana, T., Newmeyer, D. D., and Green, D. R. (2000) The 'harmless' release of cytochrome *c*. *Cell Death Differ.* **7,** 1192–1199 CrossRef Medline
66. Martinou, I., Desagher, S., Eskes, R., Antonsson, B., André, E., Fakan, S., and Martinou, J. C. (1999) The release of cytochrome *c* from mitochondria during apoptosis of NGF-deprived sympathetic neurons is a reversible event. *J. Cell Biol.* **144,** 883–889 CrossRef Medline
67. Liu, X., Moon, S. H., Jenkins, C. M., Sims, H. F., and Gross, R. W. (2016) Cyclooxygenase-2 mediated oxidation of 2-arachidonoyl-lysophospholipids identifies unknown lipid signaling pathways. *Cell Chem. Biol.* **23,** 1217–1227 CrossRef Medline
68. Moon, S. H., Jenkins, C. M., Liu, X., Guan, S., Mancuso, D. J., and Gross, R. W. (2012) Activation of mitochondrial calcium-independent phospholipase $A_2\gamma$ (iPLA$_2\gamma$) by divalent cations mediating arachidonate release and production of downstream eicosanoids. *J. Biol. Chem.* **287,** 14880–14895 CrossRef Medline
69. Heffern, C. T., Pocivavsek, L., Birukova, A. A., Moldobaeva, N., Bochkov, V. N., Lee, K. Y., and Birukov, K. G. (2013) Thermodynamic and kinetic investigations of the release of oxidized phospholipids from lipid membranes and its effect on vascular integrity. *Chem. Phys. Lipids* **175–176,** 9–19 CrossRef Medline
70. Koeberle, A., Shindou, H., Koeberle, S. C., Laufer, S. A., Shimizu, T., and Werz, O. (2013) Arachidonoyl-phosphatidylcholine oscillates during the cell cycle and counteracts proliferation by suppressing Akt membrane binding. *Proc. Natl. Acad. Sci. U.S.A.* **110,** 2546–2551 CrossRef Medline
71. Yan, W., Jenkins, C. M., Han, X., Mancuso, D. J., Sims, H. F., Yang, K., and Gross, R. W. (2005) The highly selective production of 2-arachidonoyl lysophosphatidylcholine catalyzed by purified calcium-independent phospholipase $A_2\gamma$: identification of a novel enzymatic mediator for the generation of a key branch point intermediate in eicosanoid signaling. *J. Biol. Chem.* **280,** 26669–26679 CrossRef Medline
72. Lesnefsky, E. J., Chen, Q., Tandler, B., and Hoppel, C. L. (2017) Mitochondrial dysfunction and myocardial ischemia-reperfusion: implications for novel therapies. *Annu. Rev. Pharmacol. Toxicol.* **57,** 535–565 CrossRef Medline
73. Ginsberg, L., Rafique, S., Xuereb, J. H., Rapoport, S. I., and Gershfeld, N. L. (1995) Disease and anatomic specificity of ethanolamine plasmalogen deficiency in Alzheimer's disease brain. *Brain Res.* **698,** 223–226 CrossRef Medline
74. Correia, S. C., Perry, G., and Moreira, P. I. (2016) Mitochondrial traffic jams in Alzheimer's disease—pinpointing the roadblocks. *Biochim. Biophys. Acta* **1862,** 1909–1917 CrossRef Medline
75. Moreira, P. I., Carvalho, C., Zhu, X., Smith, M. A., and Perry, G. (2010) Mitochondrial dysfunction is a trigger of Alzheimer's disease pathophysiology. *Biochim. Biophys. Acta* **1802,** 2–10 CrossRef Medline
76. Weisser, M., Vieth, M., Stolte, M., Riederer, P., Pfeuffer, R., Leblhuber, F., and Spiteller, G. (1997) Dramatic increase of α-hydroxyaldehydes derived from plasmalogens in the aged human brain. *Chem. Phys. Lipids* **90,** 135–142 CrossRef Medline
77. Hagihara, B., Morikawa, I., Tagawa, K., and Okunuki, K. (1958) Crystalline animal cytochrome c: II. crystallization of pigeon cytochrome c and a comparison of two crystallization methods. *J. Biochem.* **45,** 565–574 CrossRef
78. Creer, M. H., and Gross, R. W. (1985) Reversed-phase high-performance liquid chromatographic separation of molecular species of alkyl ether, vinyl ether, and monoacyl lysophospholipids. *J. Chromatogr.* **338,** 61–69 CrossRef Medline
79. Creer, M. H., and Gross, R. W. (1985) Separation of isomeric lysophospholipids by reverse phase HPLC. *Lipids* **20,** 922–928 CrossRef Medline
80. van Gelder, B., and Slater, E. C. (1962) The extinction coefficient of cytochrome *c*. *Biochim. Biophys. Acta* **58,** 593–595 CrossRef
81. Han, X., Yang, K., and Gross, R. W. (2012) Multi-dimensional mass spectrometry-based shotgun lipidomics and novel strategies for lipidomic analyses. *Mass Spectrom. Rev.* **31,** 134–178 CrossRef Medline
82. Folch, J., Lees, M., and Sloane Stanley, G. H. (1957) A simple method for the isolation and purification of total lipides from animal tissues. *J. Biol. Chem.* **226,** 497–509 Medline
83. Moon, S. H., Jenkins, C. M., Kiebish, M. A., Sims, H. F., Mancuso, D. J., and Gross, R. W. (2012) Genetic ablation of calcium-independent phospholipase $A_2\gamma$ (iPLA$_2\gamma$) attenuates calcium-induced opening of the mitochondrial permeability transition pore and resultant cytochrome *c* release. *J. Biol. Chem.* **287,** 29837–29850 CrossRef Medline
84. Moon, S. H., Liu, X., Cedars, A. M., Yang, K., Kiebish, M. A., Joseph, S. M., Kelley, J., Jenkins, C. M., and Gross, R. W. (2018) Heart failure-induced activation of phospholipase iPLA$_2\gamma$ generates hydroxyeicosatetraenoic acids opening the mitochondrial permeability transition pore. *J. Biol. Chem.* **293,** 115–129 CrossRef Medline
85. Yang, K., Zhao, Z., Gross, R. W., and Han, X. (2009) Systematic analysis of choline-containing phospholipids using multi-dimensional mass spectrometry-based shotgun lipidomics. *J. Chromatogr. B Analyt. Technol. Biomed. Life Sci.* **877,** 2924–2936 CrossRef Medline
86. Han, X., Yang, K., Cheng, H., Fikes, K. N., and Gross, R. W. (2005) Shotgun lipidomics of phosphoethanolamine-containing lipids in biological samples after one-step in situ derivatization. *J. Lipid Res.* **46,** 1548–1560 CrossRef Medline
87. Samhan-Arias, A. K., Ji, J., Demidova, O. M., Sparvero, L. J., Feng, W., Tyurin, V., Tyurina, Y. Y., Epperly, M. W., Shvedova, A. A., Greenberger, J. S., Bayir, H., Kagan, V. E., and Amoscato, A. A. (2012) Oxidized phospholipids as biomarkers of tissue and cell damage with a focus on cardiolipin. *Biochim. Biophys. Acta* **1818,** 2413–2423 CrossRef Medline

Cytochrome *c* is an oxidative stress−activated plasmalogenase that cleaves plasmenylcholine and plasmenylethanolamine at the *sn*-1 vinyl ether linkage

Christopher M. Jenkins, Kui Yang, Gaoyuan Liu, Sung Ho Moon, Beverly G. Dilthey and Richard W. Gross

J. Biol. Chem. 2018, 293:8693-8709.
doi: 10.1074/jbc.RA117.001629 originally published online March 12, 2018
